

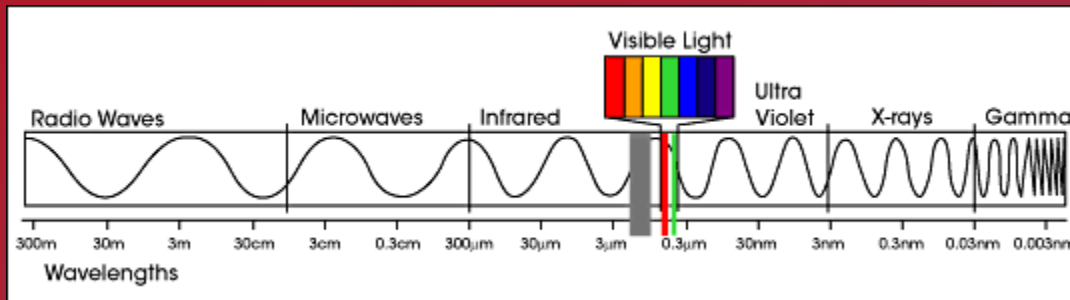
FOUNDATIONS AND APPLICATIONS OF PASSIVE AND ACTIVE INFRARED THERMOGRAPHY

Andreas Mandelis

Center for Advanced Diffusion-Wave and
Photoacoustic Technologies, University of
Toronto, Toronto, ON, M5S3G8, Canada

INFRARED BASICS

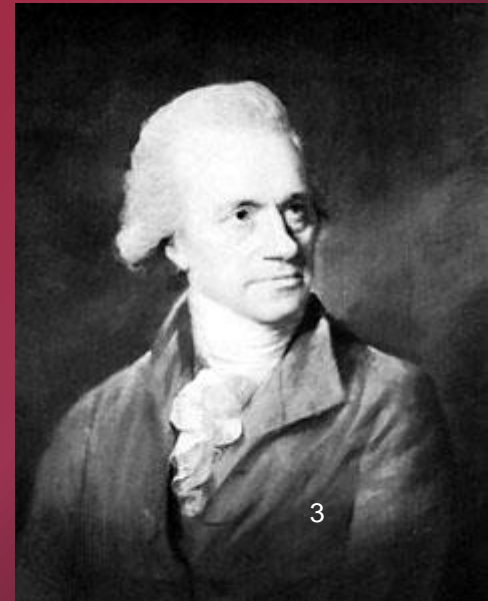
- Infrared: The portion of the electromagnetic spectrum between 700 nm and 1 mm
- Infrared \equiv “Below Red”



http://earthobservatory.nasa.gov/Experiments/ICE/panama/Images/em_spectrum.gif

INFRARED HISTORY: SIR WILLIAM HERSCHEL

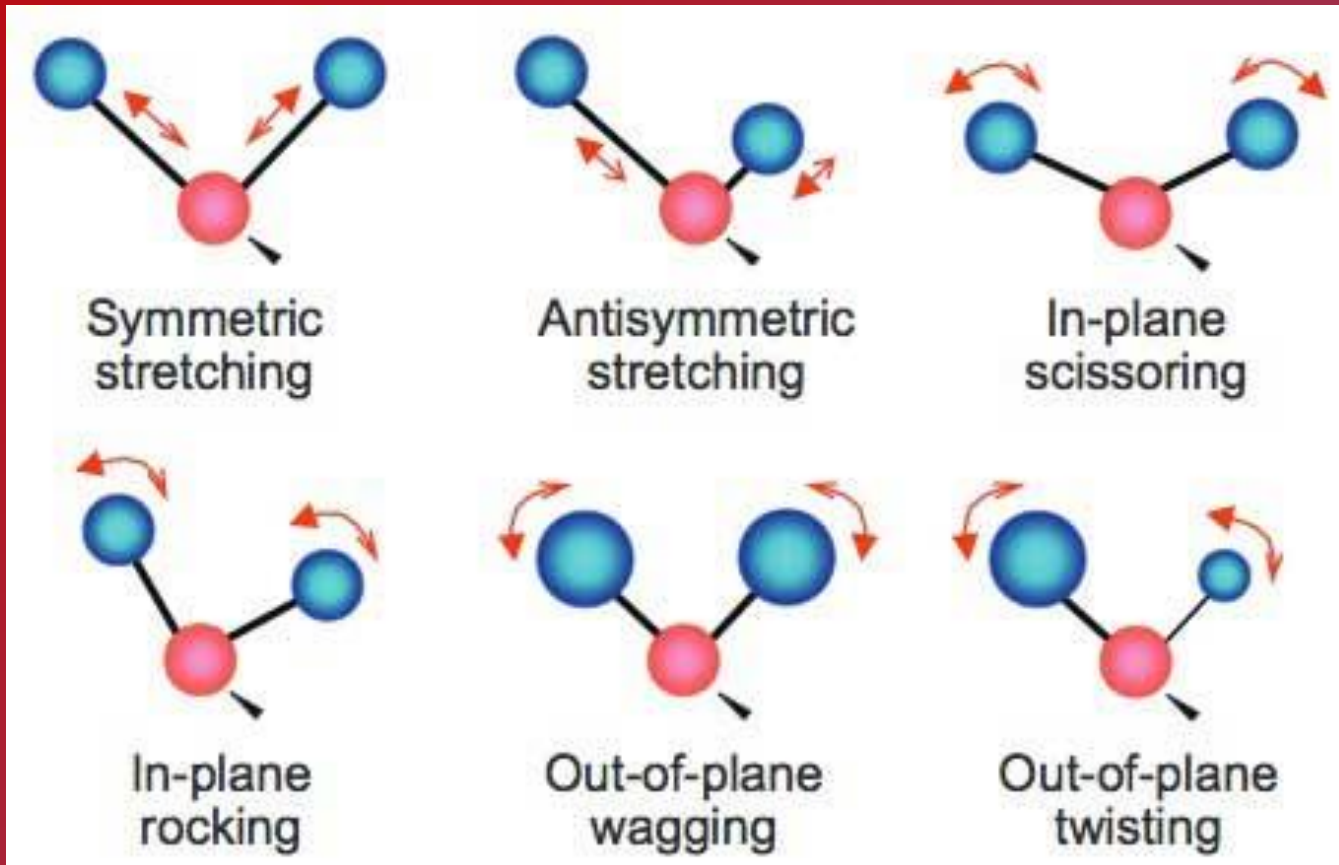
- British/German astronomer and composer
- Two experiments led to the theory of Infrared radiation in 1800
- Red filters to observe sun spots
- Prism and thermometer to observe the temperature of different colors.
- On 11 February 1800, Herschel was testing filters for the sun so he could observe sun spots. When using a red filter he found there was a lot of heat produced. Herschel discovered infrared radiation in sunlight by passing it through a prism and holding a thermometer just beyond the red end of the visible spectrum. This thermometer was meant to be a control to measure the ambient air temperature in the room. He was shocked when it showed a higher temperature than the visible spectrum. Further experimentation led to Herschel's conclusion that there must be an invisible form of light beyond the visible spectrum



INFRARED PHYSICS

- Emission of infrared photons caused by the vibration of molecules
- Molecules can have many different normal vibration modes

VIBRATION MODES OF A BENT MOLECULE



GOVERNING LAWS

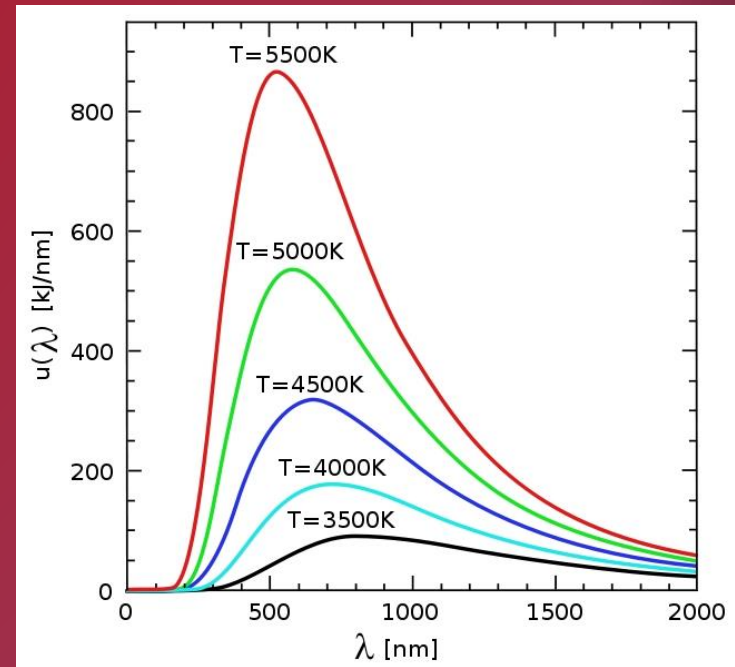
- Kirchhoff's Law of Thermal Radiation
- Wien's Displacement Law
- Planck's Law of radiative emission
- Stefan-Boltzmann Law

KIRCHHOFF'S LAW OF THERMAL RADIATION

- At thermodynamic equilibrium, a perfect blackbody absorbs all incident radiation and emits the same total energy
- The radiation emitted by the blackbody depends only on its temperature and the emitted wavelength

WIEN'S DISPLACEMENT LAW

- The wavelength at which maximum energy is emitted is inversely proportional to temperature.
- $\lambda_{\max} = b/T$
- $b = 2.8977729 \times 10^{-3} \text{ mK}$



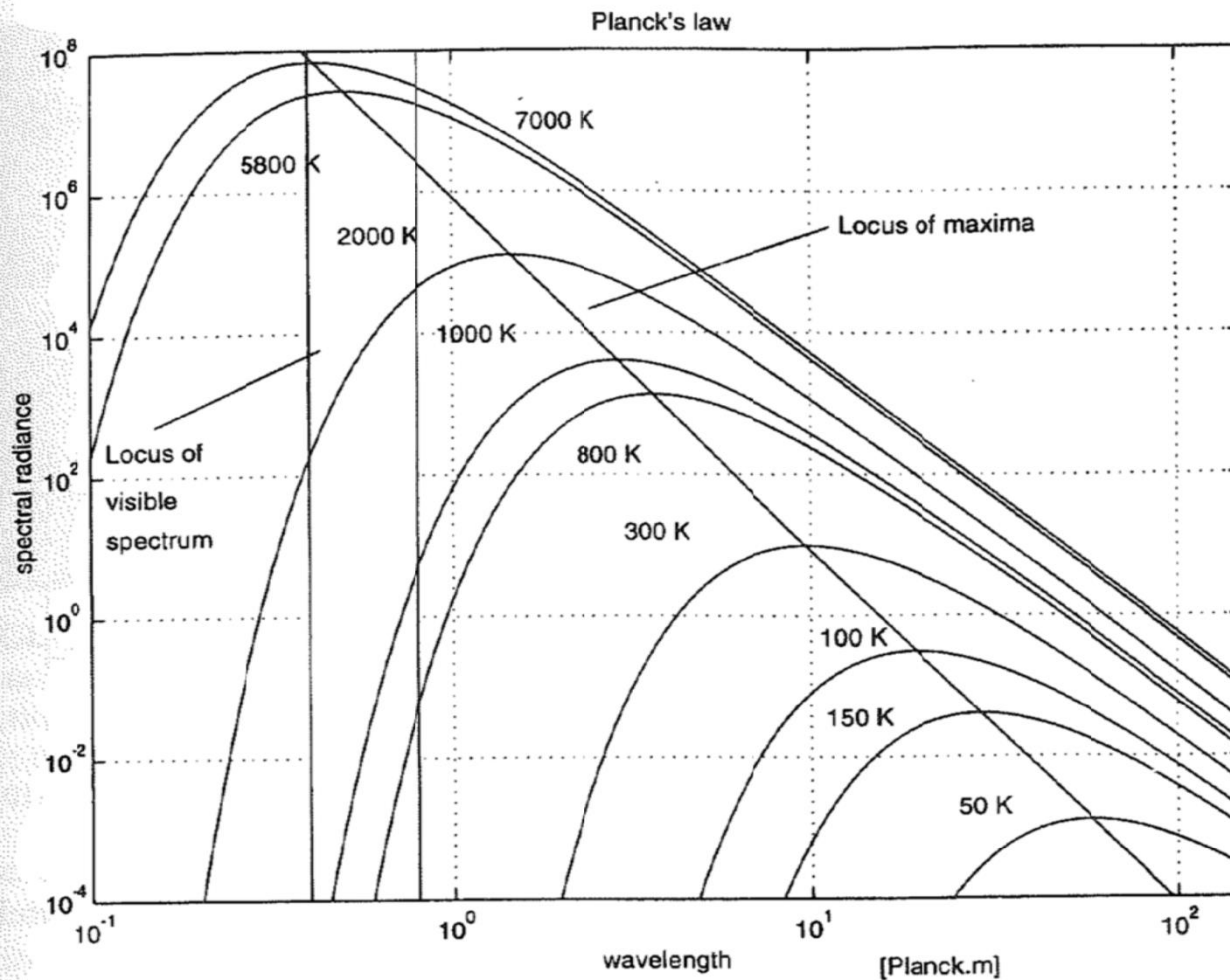


FIGURE 2.6 Spectral radiance of a blackbody (Planck's law; could be plotted with Matlab script: Planck.m).

$$L_{\lambda,b}(\lambda, T) = \frac{c_1}{\lambda^5 [\exp(c_2/\lambda T) - 1]} \quad \text{W m}^2 \mu\text{m}^{-1} \text{sr}^{-1} \quad (2.15)$$

PLANCK'S LAW

- $W_{\lambda} = \frac{2hc^2}{\lambda^5} \frac{1}{e^{\frac{hc}{\lambda kT}} - 1} \left(\frac{W}{\text{Sr m}^3} \right)$
- $E = \frac{hc}{\lambda}$ (J/photon)
- Completely describes irradiation as a function of temperature and wavelength/frequency

STEFAN-BOLTZMANN LAW

- $E = \sigma T^4$
- $\sigma = 5.6703 \times 10^{-8} \text{ W/m}^2\text{K}^4$
- Valid for blackbodies
- Across all wavelengths
- Modified to include emissivity: $E = \epsilon \sigma T^4$

BLACKBODY RADIATION FUNCTION

- Fraction of total emitted energy at a particular temperature from 0 to a certain wavelength can be determined
- Very little of the total emitted energy at room temperature is below infrared

Blackbody Radiation Functions

λT ($\mu\text{m}\cdot\text{K}$)	$F_{0\rightarrow\lambda}$				
200	0.000000	4,000	0.480877	9,000	0.890029
400	0.000000	4,200	0.516014	9,500	0.903085
600	0.000000	4,400	0.548796	10,000	0.914199
800	0.000016	4,600	0.579820	10,500	0.923710
1,000	0.000321	4,800	0.607559	11,000	0.931890
1,200	0.002134	5,000	0.633747	11,500	0.939959
1,400	0.007790	5,200	0.658970	12,000	0.945098
1,600	0.019718	5,400	0.680360	13,000	0.955139
1,800	0.039341	5,600	0.701046	14,000	0.962898
2,000	0.066728	5,800	0.720158	15,000	0.969981
2,200	0.100888	6,000	0.737818	16,000	0.973814
2,400	0.140256	6,200	0.754140	18,000	0.980860
2,600	0.183120	6,400	0.769234	20,000	0.985602
2,800	0.227897	6,600	0.783199	25,000	0.992215
2,898	0.250108	6,800	0.796129	30,000	0.995340
3,000	0.273232	7,000	0.808109	40,000	0.997967
3,200	0.318102	7,200	0.819217	50,000	0.998953
3,400	0.361725	7,400	0.829527	75,000	0.997130
3,600	0.403607	7,600	0.839102	100,000	0.999905
3,800	0.443382	7,800	0.848005		
		8,000	0.856288		
		8,500	0.875608		

1. Values from Table 12.1, Incropera and DeWitt, 1999.
 2. Constants used to generate these blackbody functions are: $C_1 = 3.7420 \times 10^8 \mu\text{m}^4/\text{m}^2$ and $C_2 = 1.4388 \times 10^4 \mu\text{m}\cdot\text{K}$.

GOVERNING LAWS AND THERMOGRAPHY

- Temperature guns (Pyrometers) use the Stefan Boltzmann Law to calculate the temperature of an object.
- $E = \epsilon\sigma T^4$
- A series of lenses focus the incoming radiation on a sensor
- The sensor converts the infrared energy to a voltage signal.



http://www.fluke.com/images/Products/Industrial/Thermometers/568_566.jpg

THE IMPORTANCE OF EMISSIVITY

- The emissivity of the surface of a material is its effectiveness in emitting energy as thermal radiation. Quantitatively, emissivity is the ratio of the thermal radiation from a surface to the radiation from an ideal black surface at the same temperature as given by the Stefan–Boltzmann law.
- $E = \epsilon\sigma T^4$
- No objects are perfect blackbodies
- Emissivity can vary from near 1 to near 0 (for very reflective materials such as silver and aluminum)
- Emissivity must be accounted for when using temperature guns or thermal cameras or significant errors can occur



THERMAL IMAGING CAMERAS

- Operation is based on the same principle as temperature guns
- Camera creates a 2D image using an array of sensors
- Behaves similar to a modern digital camera

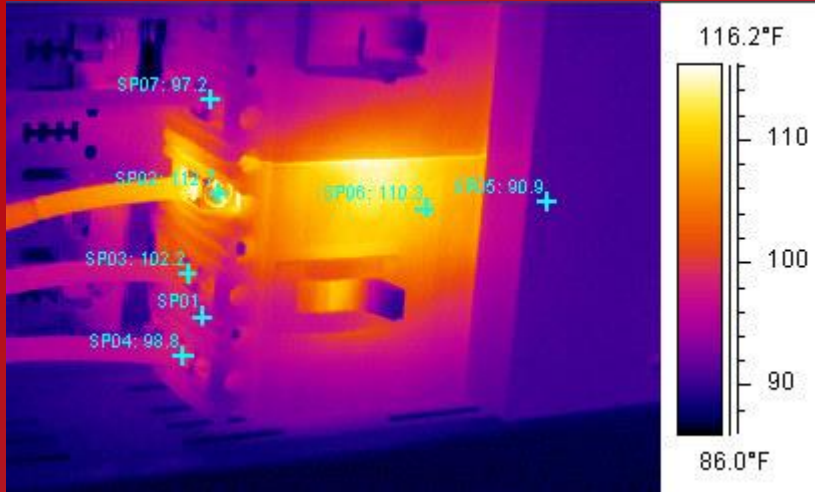


http://www.flir.ca/uploadedImages/Thermography_USA/Products/E-Series/Exx-Series-WiFi.png

PASSIVE THERMOGRAPHY

Uses infrared imaging to capture the natural temperature variations or mappings in materials and structures like buildings. It is used in the predictive maintenance community where temperature distributions of operating machinery or electrical systems are imaged to locate hot spots indicative of operating problems. This is a very important technological field and **does not involve the use of an external heating source.**

INFRARED CAMERAS



http://www.ir55.com/images/98127398127938712_new-6.jpg



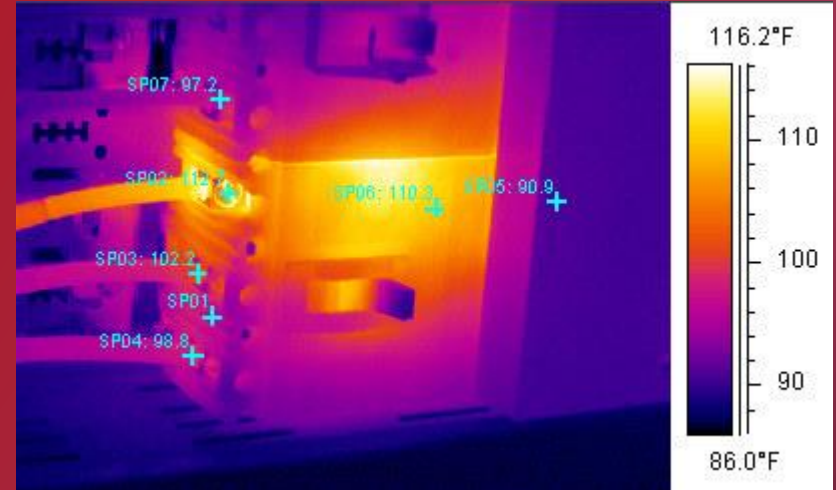
<http://thermalimagingcamera.us/wp-content/uploads/2015/06/Infrared-House.jpg>



http://www.flir.ca/uploadedImages/Thermography_USA/Products/E-Series/Exx-Series-WiFi.png

THERMAL IMAGING CAMERA USE

- Software interface shows a colored image representing the temperature gradient of the camera's field of view
- Calibrated targets can be placed on the image to determine the exact temperature
- A laser guide can be used to help aim the camera
- “Trigger” used for capturing and saving image
- Should be pointed straight at desired object if it is not a diffuse emitter



http://www.ir55.com/images/98127398127938712_new-6.jpg

INSTRUMENTATION

- Minimal: Thermal Imaging Camera
- Common brands: FLIR, Fluke, Seek Thermal, Micro-Epsilon
- Optional additions: computer software, multi-meter, moisture meter, active heating source

THERMAL IMAGING CAMERA USE

- Save pictures and/or videos (with viewing mode)
- Picture in picture mode (infrared image with visual image)
- Accuracy/sensitivity
- Temperature range
- Resolution
- Alarm mode (indicating if a temperature is measured above a desired limit)
- Multiple temperature spots
- Image editing and annotations
- GPS & compass
- Adjustable lens
- Wifi
- Camera Design
- Touch Screen
- Smartphone app

THERMOGRAPHY ALTERNATIVES

- Thermal Cameras are emerging in the fields of NDT and NDI as they are non-contact methods of temperature measurement
- Thermometers and thermocouples require contact
- Thermocouples are easy to use and do not require auxiliary power, but require contact and can be inaccurate

THERMAL IMAGING ADVANTAGES

- Large area and moving objects can be measured
- “Big Picture”
- Non-contact. Useful for hard to reach or hazardous objects
- Easy to use
- Does not require complicated setup

THERMAL IMAGING LIMITATIONS

- Other nearby objects can result in mis-measurement
- Emissivity of the material must be known
- Surface finish can affect uniformity of emissivity
- Very dependent on the environment
- Needs to be calibrated
- Results in some inaccuracy
- Expensive

APPLICATIONS

- Building inspection
- Electrical and mechanical maintenance
- Optical gas imaging
- Night Vision
- Military and police
- Firefighting
- Medicine
- Astronomy

BUILDING INSPECTION

- Heating and cooling require the most energy compared to other home energy uses
- Insufficient insulation and/or moisture can lead to heat loss

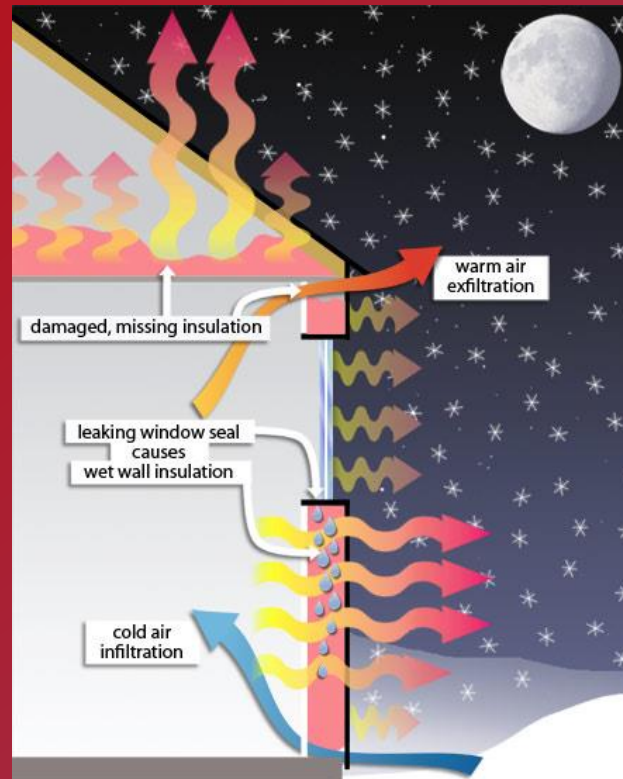


26

WHY USE THERMAL IMAGING?

- Non-Destructive: Alternatives require opening walls to inspect insulation
- Big Picture: Can scan large areas at once, making it easy to find leaks
- Safe: Does not emit any harmful rays
- Simple to understand

RESIDENTIAL HEAT LOSS



CAUSES OF INSULATION DEFECTS

- Insulation effectiveness is defined by its R value; $R = (\text{thickness of the component}) / (\text{apparent thermal conductivity})$. Larger R values mean better insulation
- Often issues arise in attics and roofs
- Missing or compressed insulation affects R value
- Poor vapor barriers can introduce moisture



29

BENEFITS OF DETECTING HEAT LOSS

- Climate control
- Energy savings
- Energy bill reduction
- Environmental benefits



<http://www.offthegridnews.com/wp-content/uploads/2016/01/power-grid-bardDOTedu.jpg>

THERMAL IMAGING AND HEAT LOSS

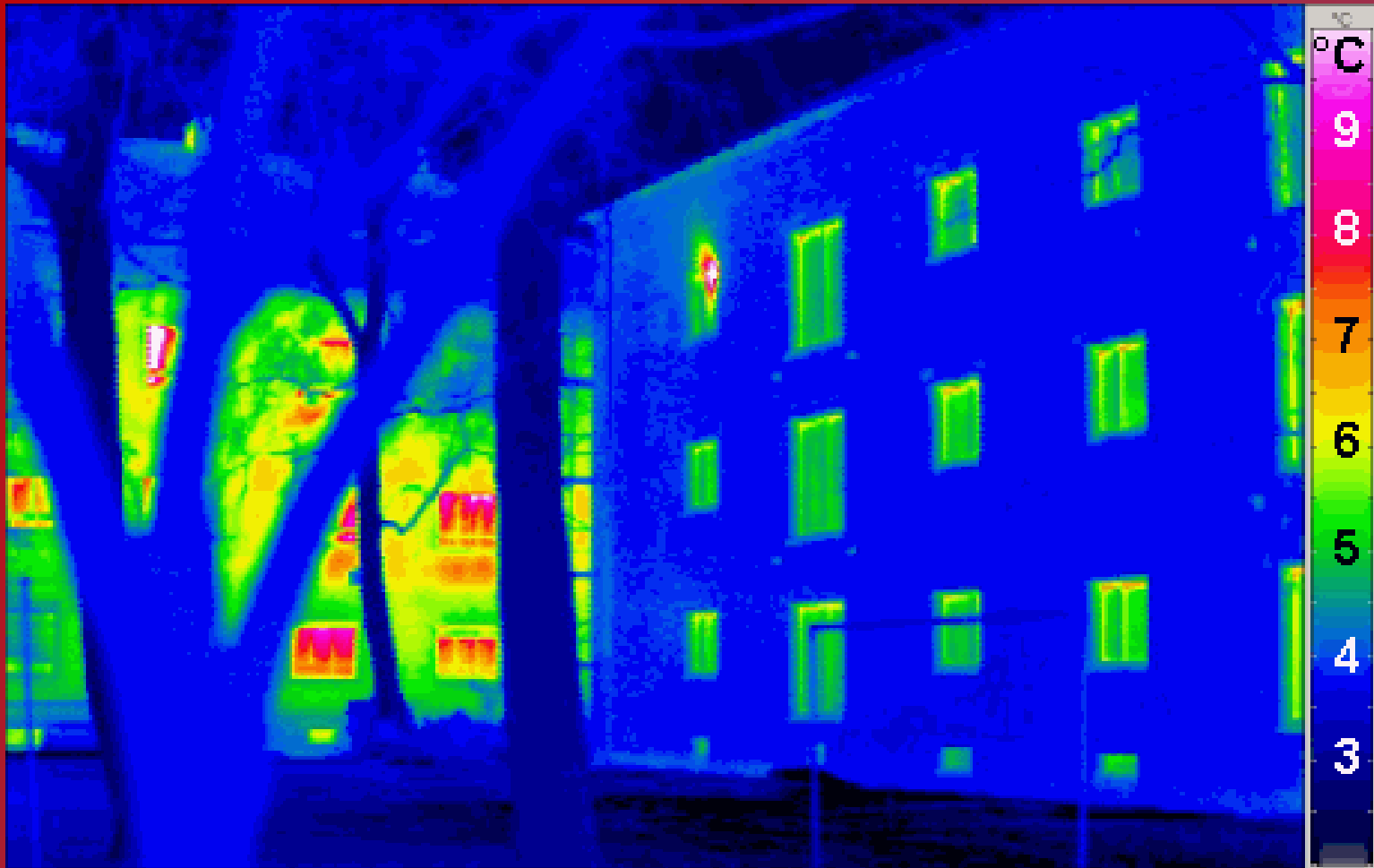
- Infrared cameras create a visual image of the temperature distribution of the façade of a house (or interior room)
- Exterior: The warmest portion of the outer walls indicates heat losses
- Interior: The coolest portion of an inner wall indicates where heat is lost



<http://thermalimagingcamera.us/wp-content/uploads/2015/06/Infrared-House.jpg>



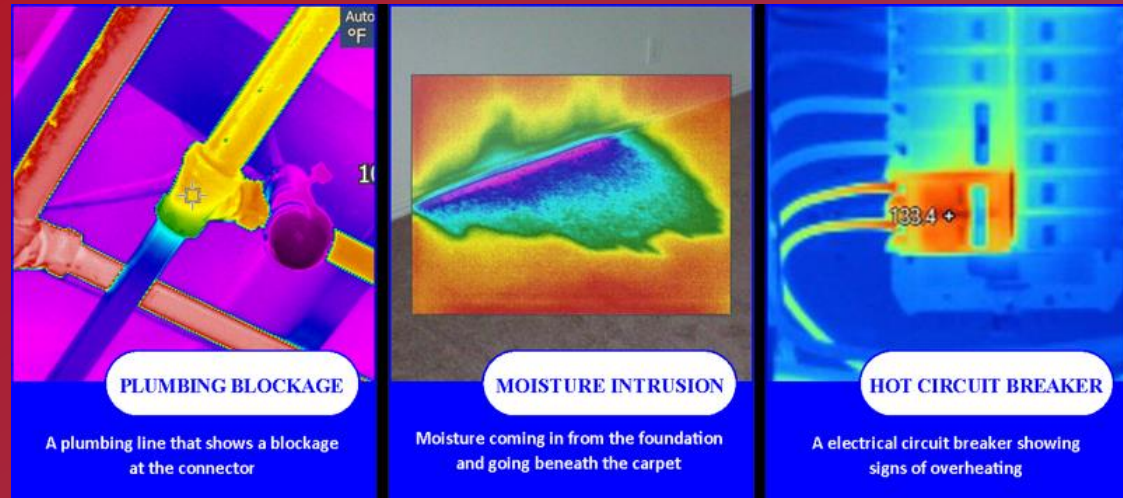
<http://www.infrarednewengland.com/wp-content/uploads/2010/08/residential-heat-loss-IR-scan.jpg>



https://upload.wikimedia.org/wikipedia/commons/f/f2/Passivhaus_thermogram_gedaemmt_ungeaedemmt.png

THERMAL IMAGING AND OTHER BUILDING APPLICATIONS

- Locate moisture to avoid heat loss and health concerns
- Analyze HVAC flow
- Determine the location of inner wall components prior to construction



HOT & COLD DRINKS IN CUPS

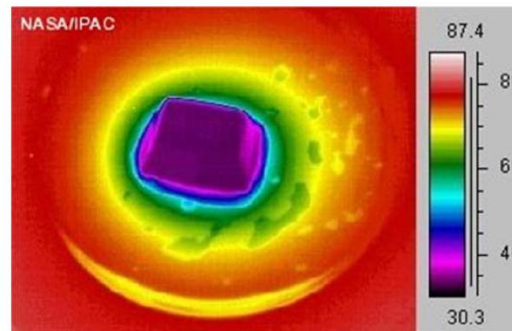
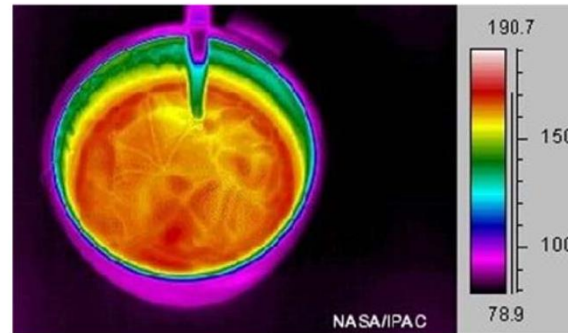


FIGURE T10: **On top** is an infrared image of a metal cup holding a very hot drink. Notice the rings of color showing heat traveling from the liquid through the metal cup. You can see this in the metal spoon as well. **On bottom** is an infrared image of a melting ice cube. Notice the rings of color showing how the melt water warms as it travels away from the cube. Although the ice cube is cold, it still puts out heat, as you can see by matching the color of the ice cube with its temperature.

HOT & COLD DRINKS, CONT'D

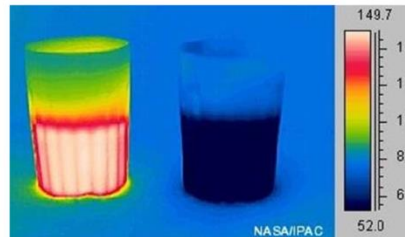


FIGURE T11: A visible light picture (**top**) and an infrared picture (**bottom**) of two cups. One cup contains cold water, while the other contains hot water. In the visible light picture we cannot tell, just by looking, which cup is holding cold water and which is holding hot water. In the infrared image, we can clearly "see" the glow from the hot water in the cup to the left and the dark, colder water in the cup to the right. If we had infrared eyes, we could tell if an object was hot or cold without having to touch it.

DEER IN FOREST AT NIGHT



FIGURE T12: By using special infrared cameras, we can get a view of the infrared world. These cameras are very useful and have even helped save people's lives. In the infrared, you can "see" in the dark. Even if the Sun is down and the lights are off, the world around us still puts out some heat. The infrared picture shows deer in a forest during a dark night. Notice how we can clearly see the heat from the deer, especially from areas not covered with thick fur like the ears, face and legs. The trees and the ground put out less heat than the deer, but can still be seen through an infrared camera.

DOG & CATERPILLAR

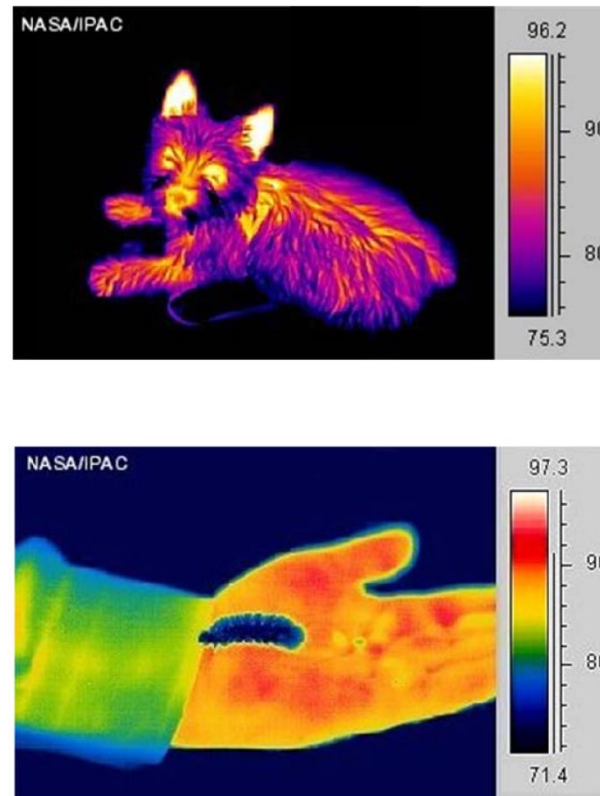


FIGURE T13: Infrared images of a warm-blooded dog (top) and of a warm-blooded human holding a cold-blooded caterpillar (bottom).

IR THROUGH PLASTIC



FIGURE T14: Above is a visible (**top**) and infrared (**bottom**) view of a person's hand inside a black plastic bag. In the visible image, the hand cannot be seen. In the infrared image, however, the heat from the hand can travel through the bag and can be seen by an infrared camera. Infrared light can pass through many materials which visible light cannot pass through.

EARTH & COSMIC IR THERMOGRAPHY

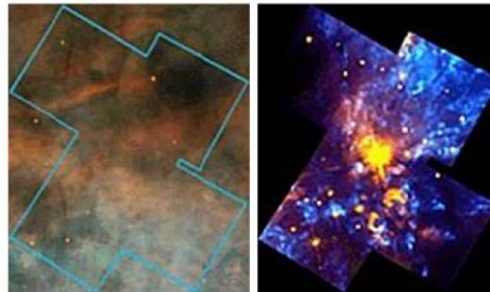
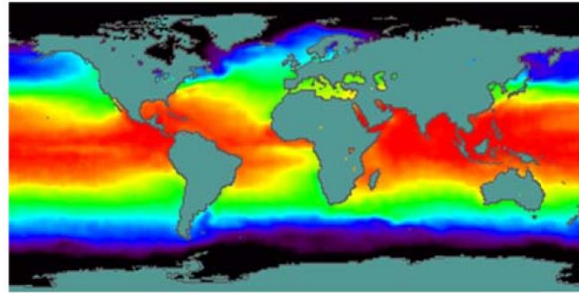


FIGURE T15: Top: An infrared map of sea surface temperatures, with red being the warmest and purple the coldest. **Bottom:** two images taken by telescopes of a thick area of gas and dust in space where stars are born. Since infrared can travel through thick dust, astronomers can see through thick clouds of dust and gas in space by using infrared telescopes. **On the left** is a space cloud as seen by a visible light telescope. Notice that we cannot see what lies behind the cloud. In the infrared view (**right**) we can see through the cloud and find bright, young stars which have just been formed.

ACTIVE THERMOGRAPHY

Active (or dynamic) thermography integrates infrared imaging with time variant external heating to assess subsurface structures via the thermal-wave response of the sample. Here camera use is more complicated than in passive thermography. The most important variant to-date is “lock-in thermography (LIT)” and advanced variants like the thermal-wave radar (TWR).

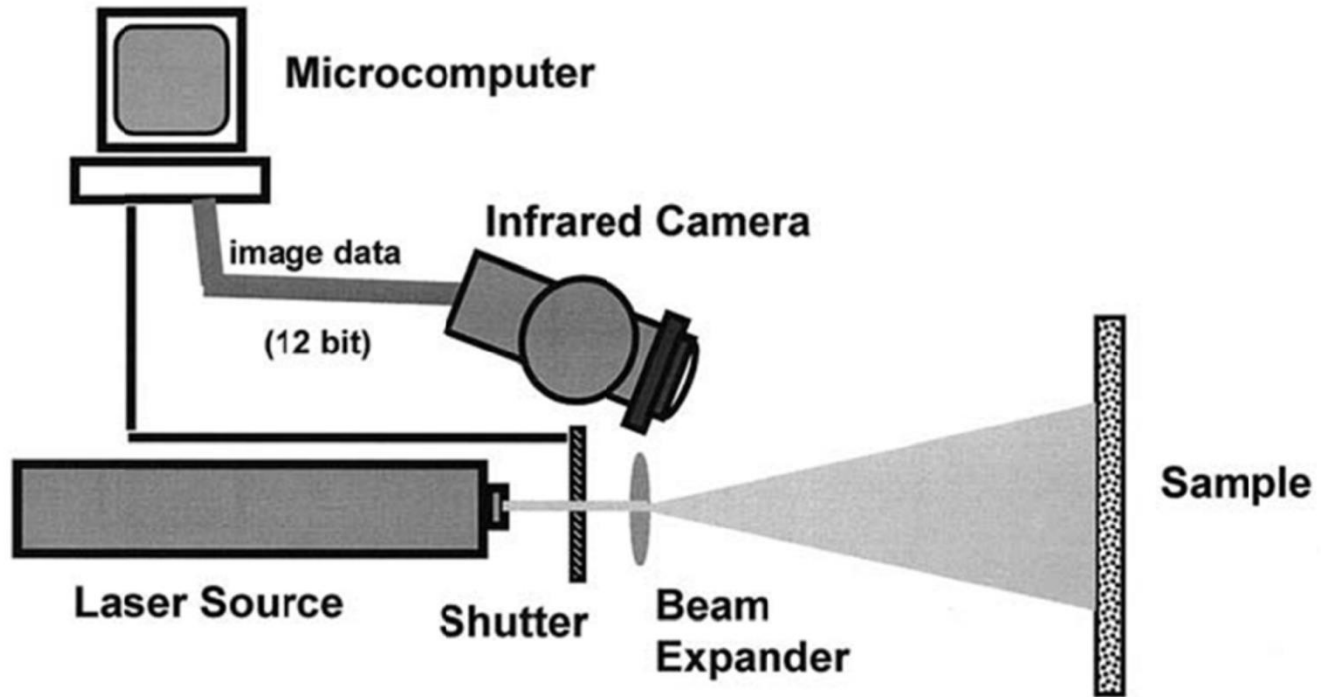


FIGURE T16: A typical experimental setup for active thermography.

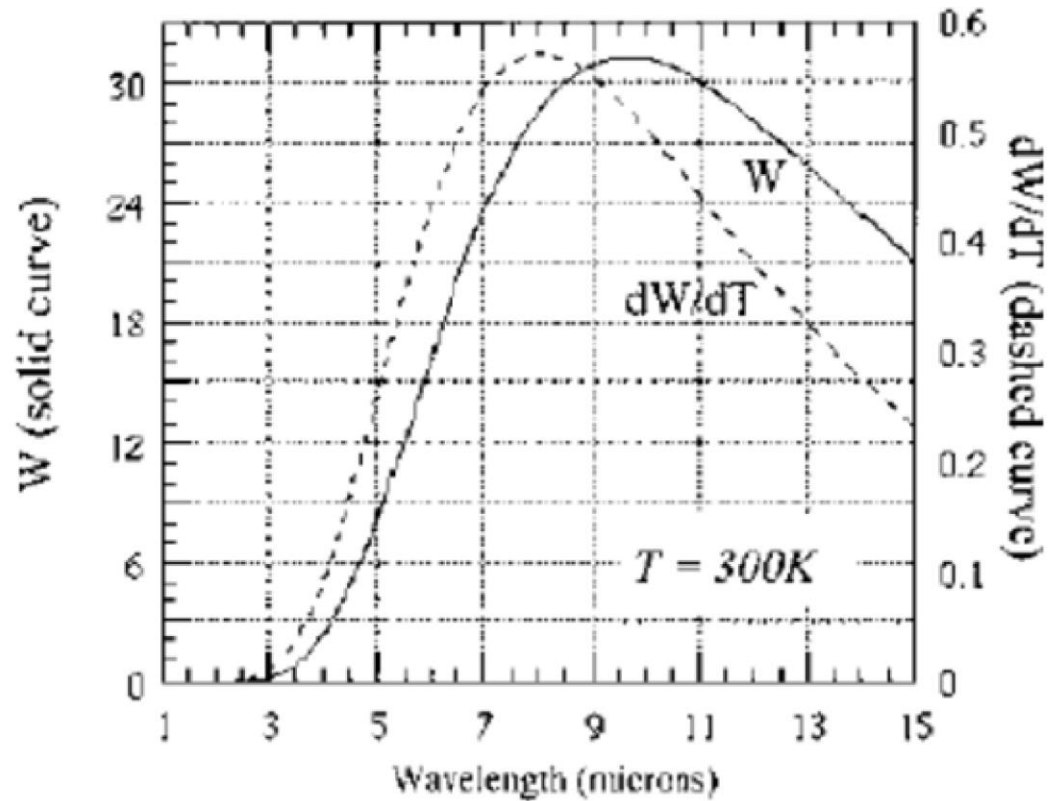


FIGURE T18. The function dW_λ/dT as a function of wavelength.

CAMERA OPTIONS

- Most basic model: FLIR E4
- $\pm 2^{\circ}C$ degrees accuracy
- 80 x 60 pixels
- $0.15^{\circ}C$ sensitivity
- $(-20^{\circ}C) - (250^{\circ}C)$ temperature range
- Higher end models have better sensitivities, temperature ranges, resolution and include more features

METHODS FOR SPECIMEN HEATING

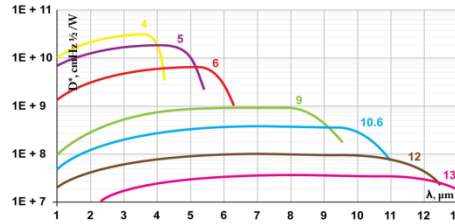
Method	Wavelength	Onset Time	Periodic Modulation Possible?
Laser	0.5–10 μm	psec–sec	✓
Flashlamps	IR	< msec	×
Quartz lams	IR	> sec	✓
Microwaves	1 mm–10 cm	> nsec	✓
Induction heating	10 cm–1 m	> msec	✓
Resistive heating	N/A	> msec	✓
Hot air blower	N/A	≫ sec	×

NON-CAMERA MID-IR DETECTORS



PC-2TE Series

2 – 13 μm IR PHOTOCONDUCTORS THERMOELECTRICALLY COOLED



Example of D^* vs Wavelength λ for PC-2TE Series HgCdTe Detectors. Spectral Characteristics of individual detectors may vary from those shown on the chart.

Features

- High performance in the 2 to 13 μm spectral range
- Fast response
- Convenient to use
- Wide dynamic range
- Compact, rugged and reliable
- Low cost
- Prompt delivery
- Custom design upon request

Description

The **PC-2TE- λ_{opt}** photodetectors series (λ_{opt} - optimal wavelength in micrometers) feature IR photoconductive detector on two-stage thermoelectrical cooler. The devices are optimized for the maximum performance at λ_{opt} . Cut-on wavelength is limited by GaAs transmittance (~0.9 μm). Bias is needed to operate photocurrent. Performance at low frequencies (<20 kHz) is reduced due to 1/f noise. Highest performance and stability are achieved by application of variable gap (HgCd)Te semiconductor, optimized doping and sophisticated surface processing. Custom devices with quadrant cells, multielement arrays, different windows, lenses and optical filters are available upon request. Standard detectors are available in **TO8** packages with wedged **BaF₂** windows. Other packages, windows and connectors are also available.

IR Detector Specification @20°C

Parameter	Symbol	Unit	PC-2TE-4	PC-2TE-5	PC-2TE-6	PC-2TE-9	PC-2TE-10.6	PC-2TE-12	PC-2TE-13
Optimal Wavelength	λ_{opt}	μm	4	5	6	9	10.6	12	13
Detectivity D^* @ λ_{peak} , 20 kHz	D^*	$\frac{cm^2 \cdot Hz^{1/2}}{W}$	$\geq 3.2 \times 10^{10}$	$\geq 2.0 \times 10^{10}$	$\geq 6.0 \times 10^9$	$\geq 9.0 \times 10^8$	$\geq 4.0 \times 10^8$	$\geq 1.0 \times 10^8$	$\geq 4.0 \times 10^7$
Voltage Responsivity - Width Product @ λ_{opt} 1x1mm	$R_v \cdot w$	$\frac{V \cdot mm}{W}$	≥ 1000	≥ 500	≥ 70	≥ 5	≥ 1.5	≥ 0.5	≥ 0.25
Time Constant	τ	ns	≤ 4000	≤ 2000	≤ 1000	≤ 20	≤ 10	≤ 2	≤ 2
Corner Frequency	1/f	kHz				1 to 20			
Bias Current - Width Ratio	$\frac{I_b}{w}$	$\frac{mA}{mm}$	1 to 2	2 to 4	4 to 8	4 to 10		5 to 15	
Sheet Resistance	R_{sh}	Ω/\square	600 to 1500	300 to 500	200 to 400	80 to 200	50 to 150	60 to 100	40 to 120
Operating Temperature	T	K				-230			
Acceptance Angle, F/#	Φ , -	deg, -				70, 0.87			

Data Sheet states minimum guaranteed D^ values for each detector model. Higher performance detectors can be provided upon request.

Type	Optical Area [mm×mm]									
	0.025×0.025	0.05×0.05	0.1×0.1	0.2×0.2	0.25×0.25	0.5×0.5	1×1	2×2	3×3	4×4
PC-2TE-4	X	X	X	X	X	X	X	X		
PC-2TE-5	X	X	X	X	X	X	X	X		
PC-2TE-6	X	X	X	X	X	X	X	X		
PC-2TE-9	X	X	X	X	X	X	X	X		
PC-2TE-10.6	X	X	X	X	X	X	X	X		
PC-2TE-12	X	X	X	X	X	X	X	X		
PC-2TE-13	X	X	X	X	X	X	X	X		

X - standard detectors

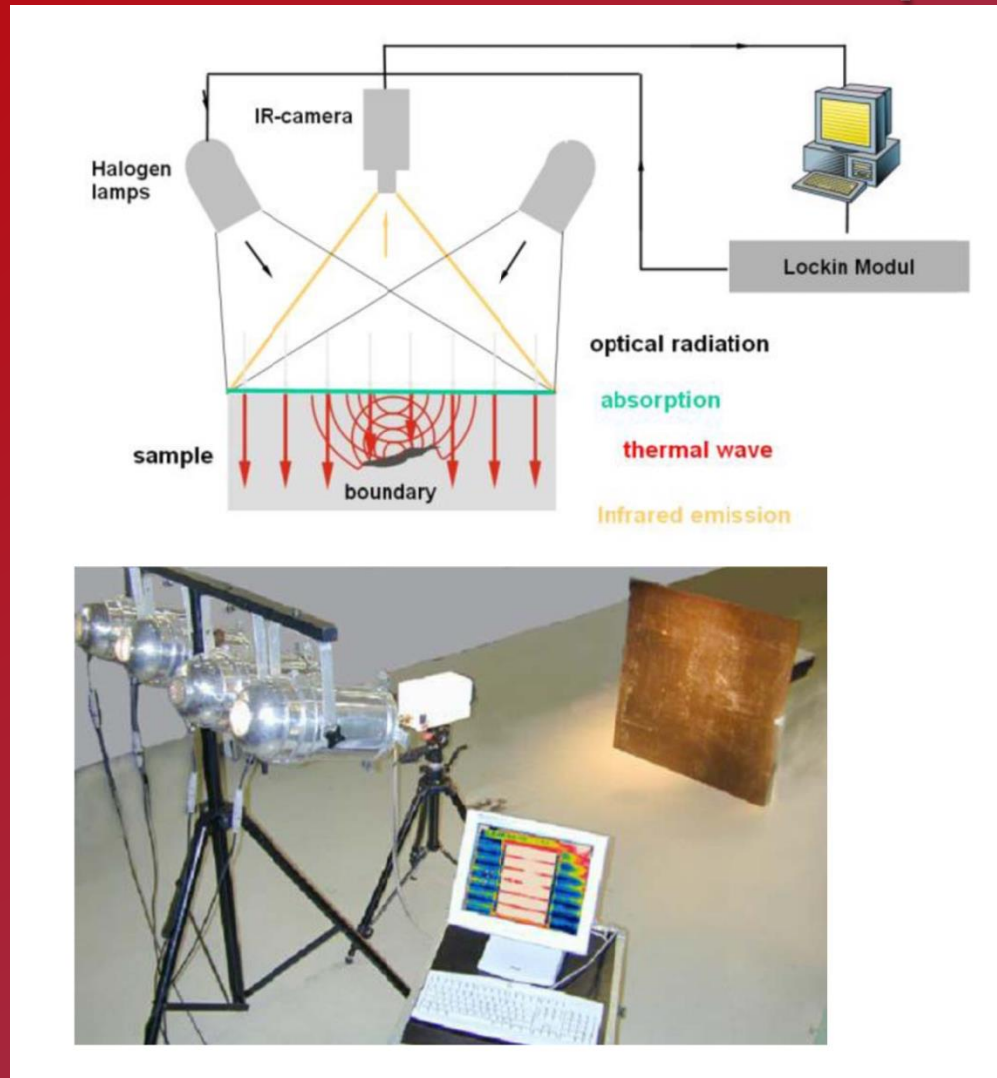
LOCK-IN THERMOGRAPHY

- Another name for lock-in thermography is modulated thermography
- The signal resolution can be improved considerably by using the lock-in principle
- Lock-in Thermography allows better contrast for inspection
- less sensitive to environmental conditions
- Phase is less sensitive/insensitive to surface emissivity

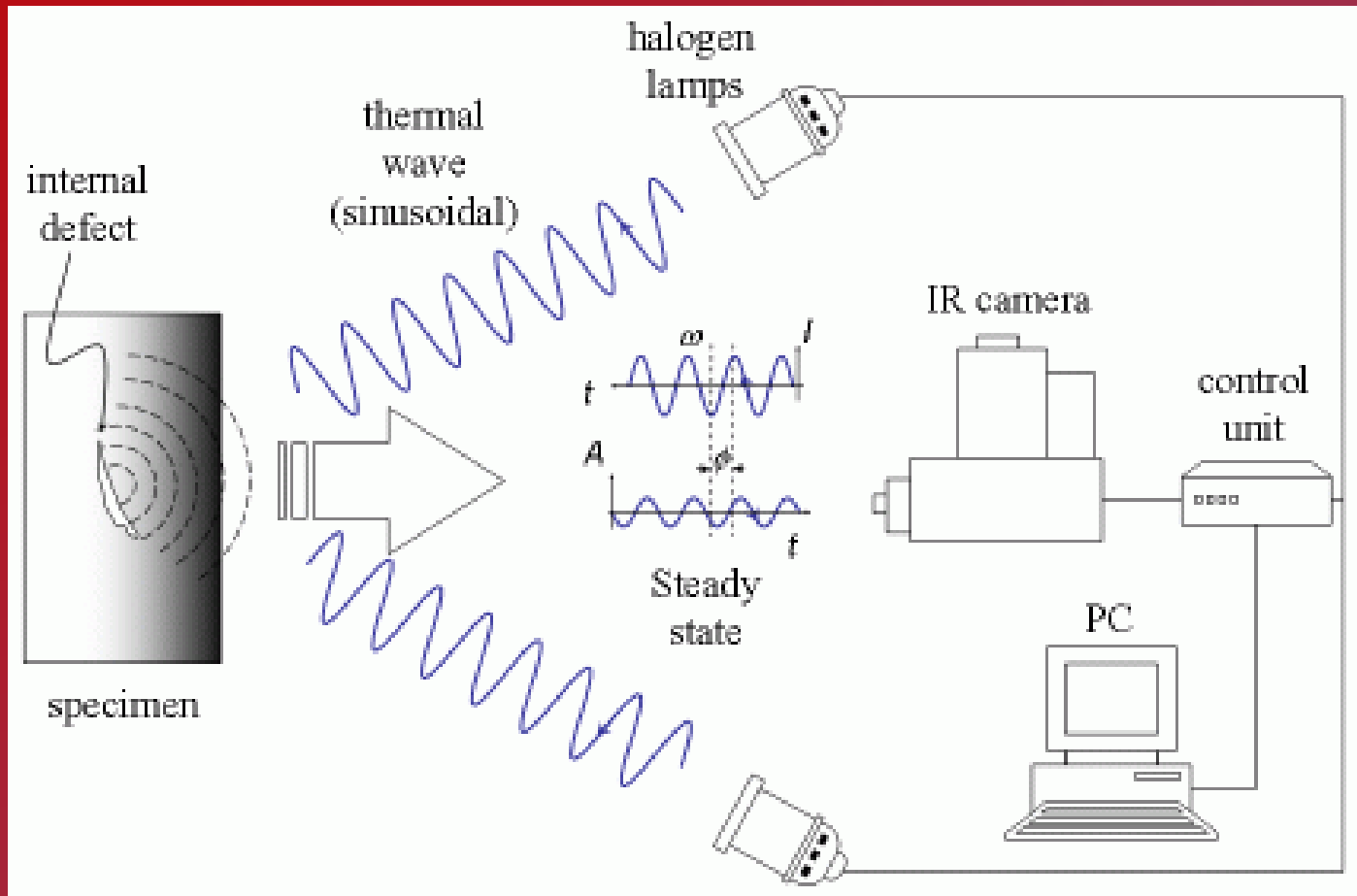
IMPROVED RESOLUTION

- Microscopic IR thermography has resolution on the order of 40 mK
- AGEMA Thermovision 900 mirror scanner, showed a noise level of 15 mK

EXERIMENTAL SET-UP FOR LOCK- IN THERMOGRAPHY (LIT)

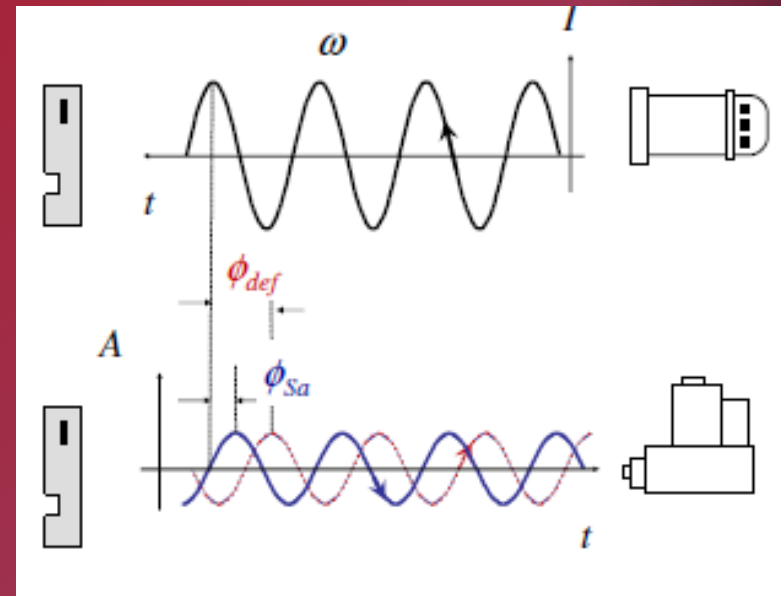


PHYSICAL PRINCIPLE OF LOCK-IN THERMOGRAPHY



SINUSOIDAL WAVE EXCITATION

- Sinusoidal waves are commonly used as trigger and as thermal excitation source (thermal wave generators)
- Shape and frequency of the response are preserved
- Only Amplitude and Phase change
- Optical- halogen lamps



SIGNAL GENERATION IN LIT

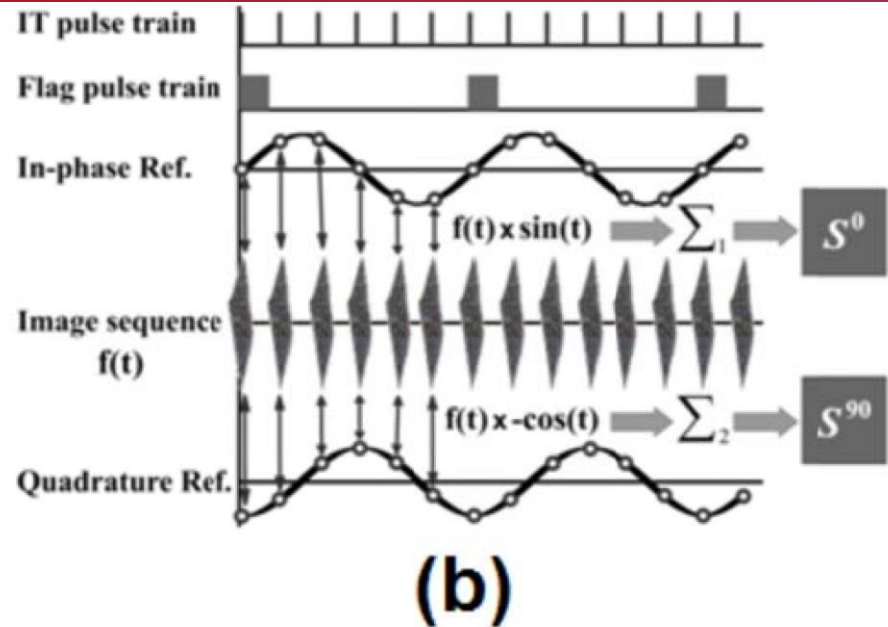
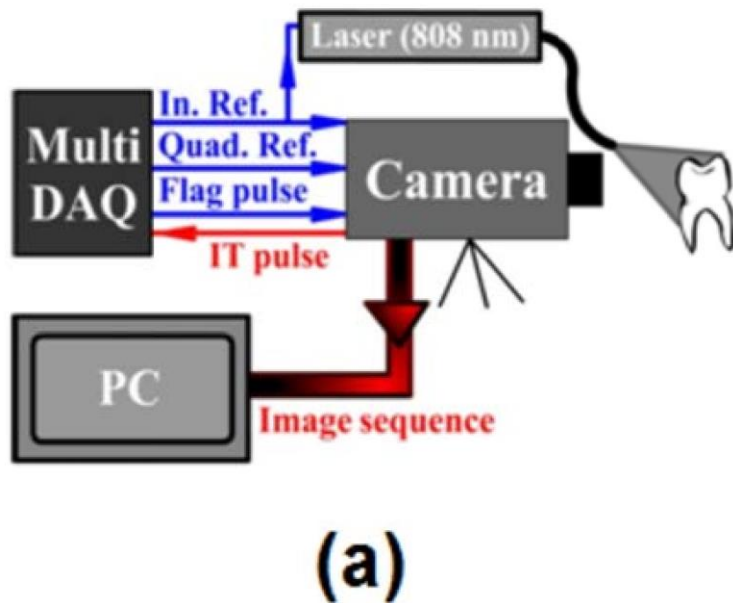
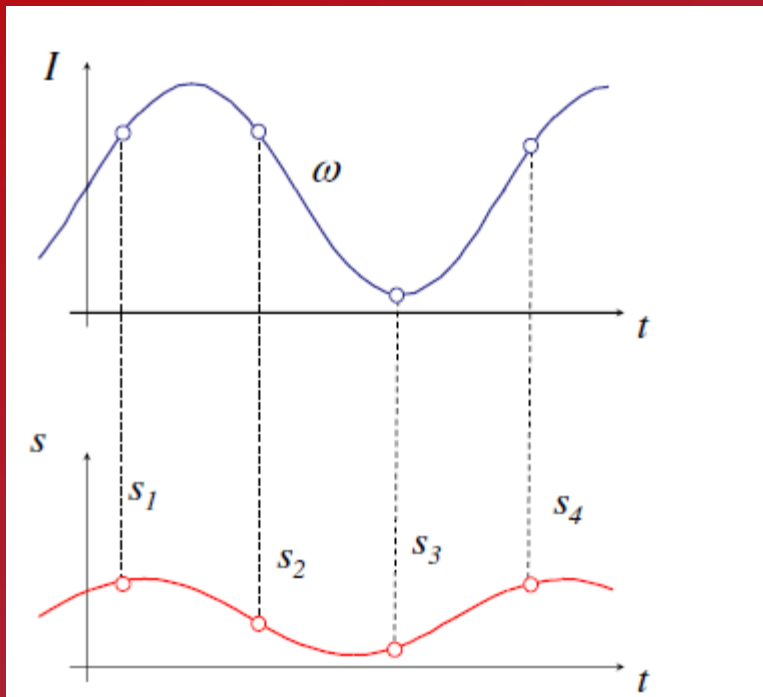


Figure T25. (a) A schematic of the thermophotonic setup along with (b) the Lock-In signal processing algorithm.

SAMPLING WAVEFORMS: FOUR POINT METHODOLOGY



$$A = \sqrt{(S_1 - S_3)^2 + (S_2 - S_4)^2}$$

$$\phi = \arctan\left(\frac{S_1 - S_3}{S_2 - S_4}\right)$$

SHANNON-NYQUIST SAMPLING THEOREM

“If a function $x(t)$ contains no frequencies higher than B hertz, it is completely determined by giving its ordinates at a series of points spaced $1/(2B)$ seconds apart”.

HIGH-FREQUENCY LIT THROUGH SYNCHRONOUS UNDERSAMPLING

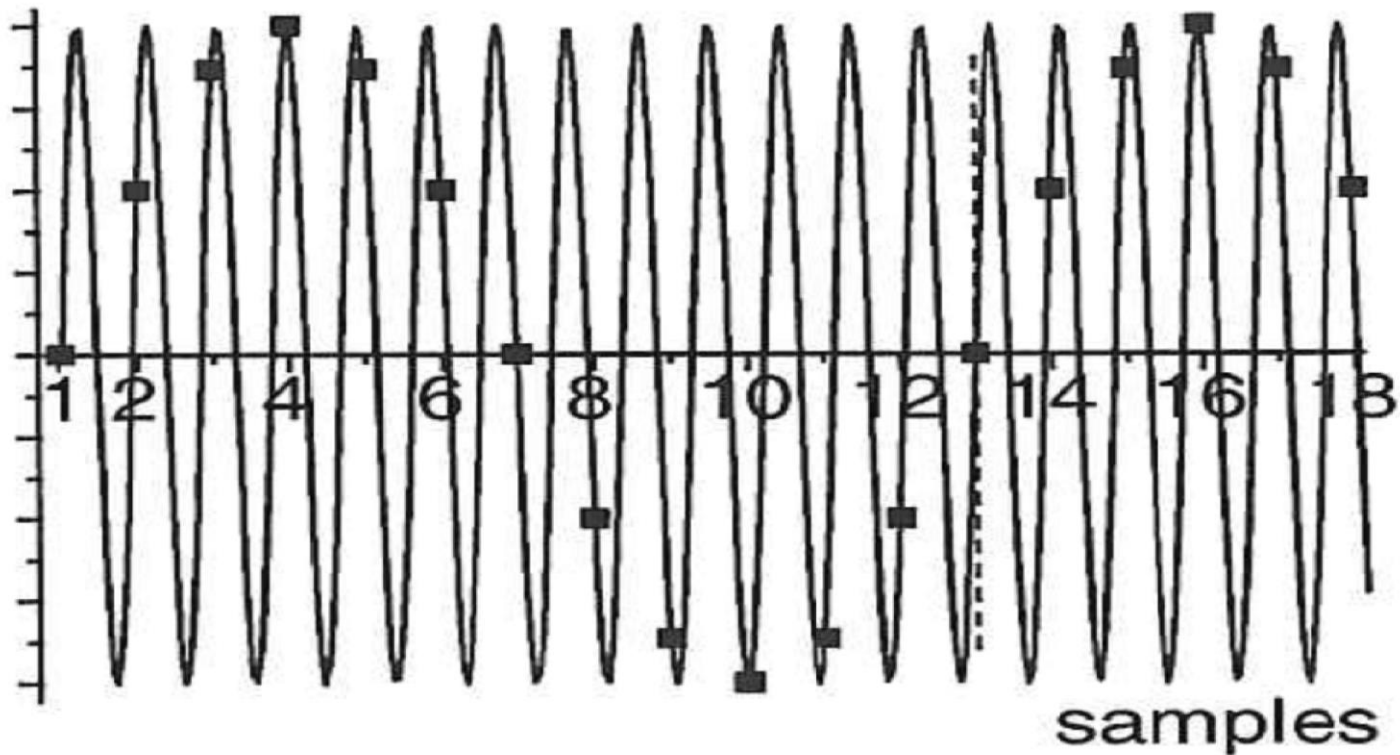


Figure T26: Synchronous undersampling of a high frequency wave form using a low sampling rate. One modulation cycle is sampled out of each 12 consecutive cycles.

DISCRETE FOURIER TRANSFORM (DFT)

$$F_n = \Delta t \sum_{k=0}^{N-1} T(k\Delta t) \exp(-j2\pi mk/N) = \text{Re}_n + \text{Im}_n$$

$$A_n = \sqrt{\text{Re}_n^2 + \text{Im}_n^2}$$

$$\phi_n = \tan^{-1}\left(\frac{\text{Im}_n}{\text{Re}_n}\right)$$

- Where j is the imaginary unit
- n is the frequency increment
- Δt is the sampling interval
- Re and Im are the real and imaginary parts of the transform

DATA FORMAT IN ACTIVE THERMOGRAPHY

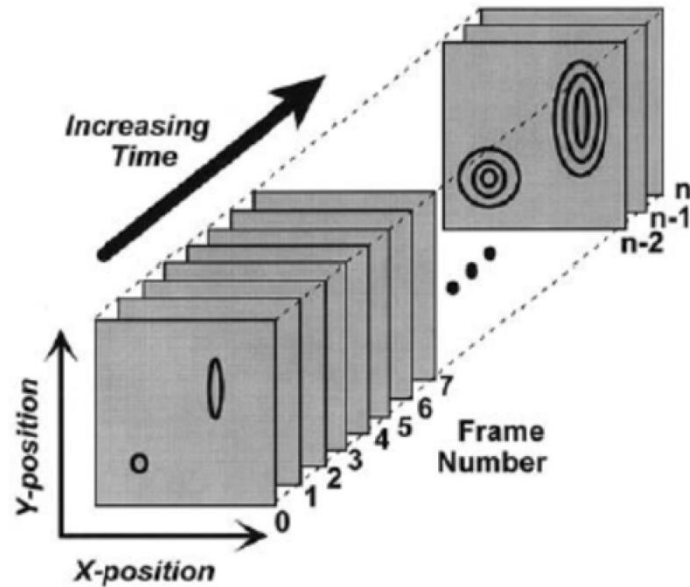


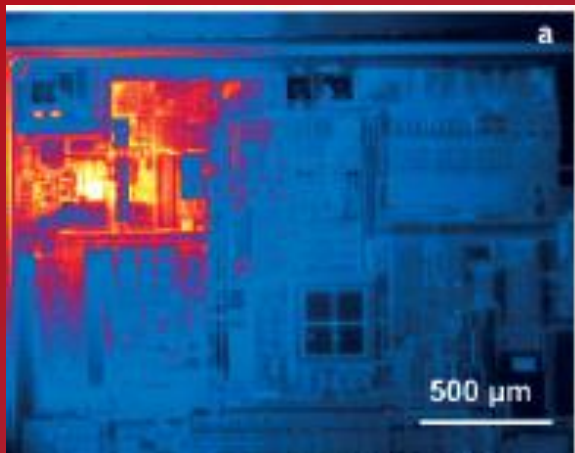
FIGURE T 23: Schematic for data format used in active thermography.

LIT ADVANTAGES AND DISADVANTAGES

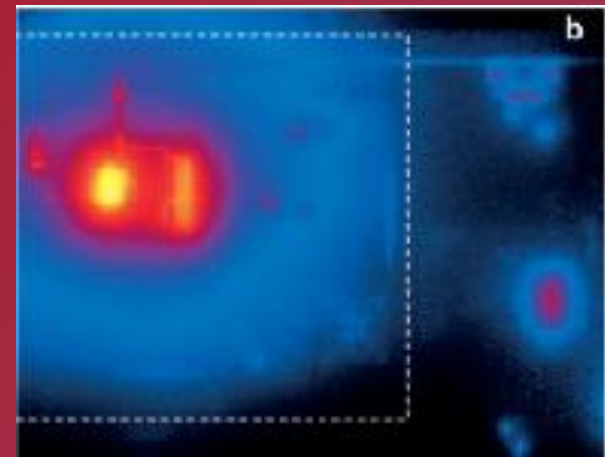
- High resolution
- Less sensitive to noise than dc thermography
- Requires less energy to perform LIT experiments
- Generally slower than other approaches

DETECTION OF HEAT SOURCES IN ELECTRONIC PACKAGING

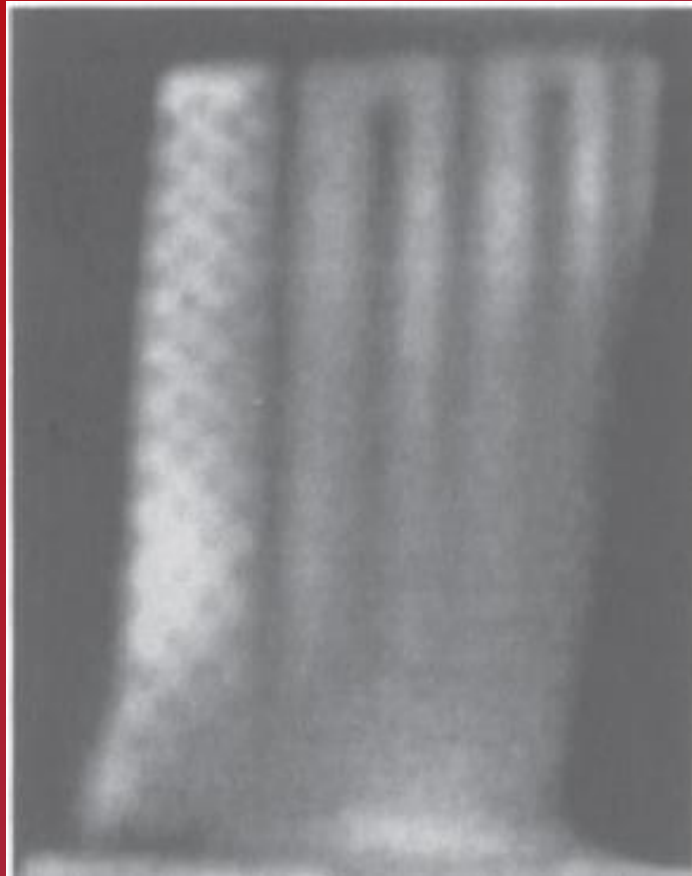
Amplitude image



Phase image

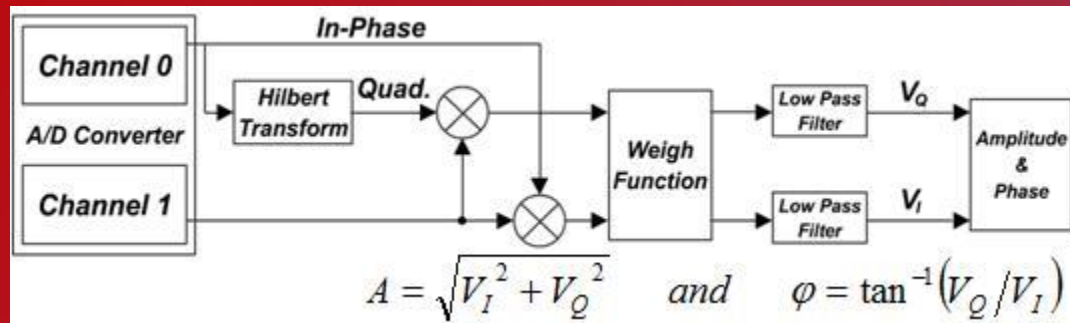


INSPECTION OF TURBINE BLADE



- **SINGLE-FREQUENCY
THERMAL-WAVE RADAR:
A NEXT GENERATION
DYNAMIC
THERMOGRAPHY**

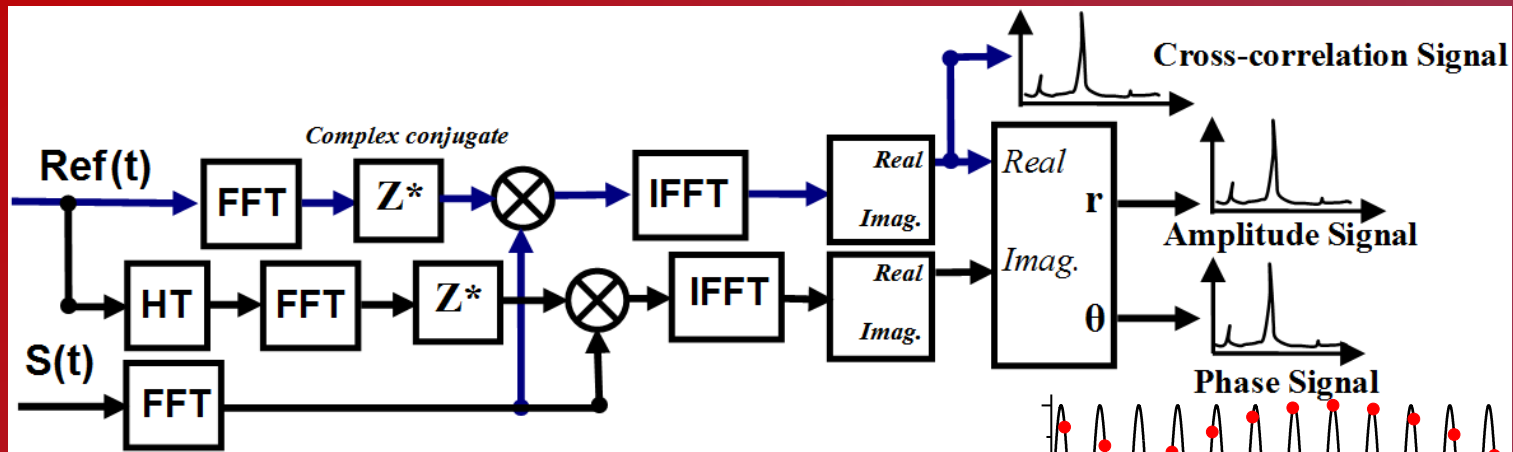
Conventional Lock-In Amplifier (LIA) signal processing.



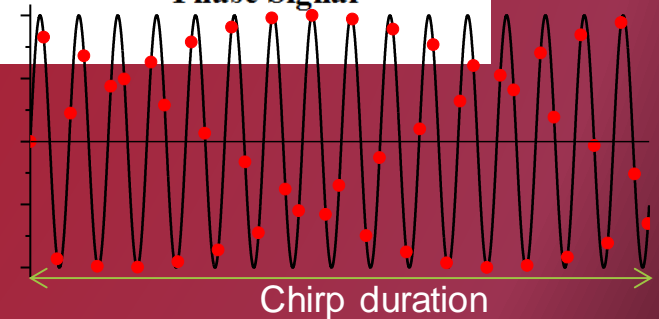
$$\begin{aligned}
 & \begin{cases} \sin(\omega_o t) \times A \sin(\omega_o t + \phi) \\ \sin(\omega_o t + 90) \times A \sin(\omega_o t + \phi) \end{cases} \xrightarrow{\text{Mixing}} \begin{cases} \frac{A}{2} [\cos(\phi) - \cos(2\omega_o t + \phi)] \\ \frac{A}{2} [\sin(\phi) - \cos(2\omega_o t + \phi + 90)] \end{cases} \xrightarrow[\times\sqrt{2}]{\text{Weighting}} \\
 & \begin{cases} \frac{A}{\sqrt{2}} [\cos(\phi) - \cos(2\omega_o t + \phi)] \\ \frac{A}{\sqrt{2}} [\sin(\phi) - \cos(2\omega_o t + \phi + 90)] \end{cases} \xrightarrow{\text{LPF}} \begin{cases} X = \frac{A}{\sqrt{2}} \cos(\phi) \\ Y = \frac{A}{\sqrt{2}} \sin(\phi) \end{cases} \rightarrow \begin{cases} A = \sqrt{X^2 + Y^2} \\ \phi = \arctan\left(\frac{Y}{X}\right) \end{cases}
 \end{aligned}$$

where $\sin(\omega_o t)$ and $\sin(\omega_o t + 90)$ represent the in-phase and quadrature reference signals and $A \sin(\omega_o t + \phi)$ is the captured infrared signal with amplitude A and phase ϕ .

Single-Frequency Thermal-Wave Radar Imaging (SF-TWRI) Signal Processing



Single frequency TWRI sampling



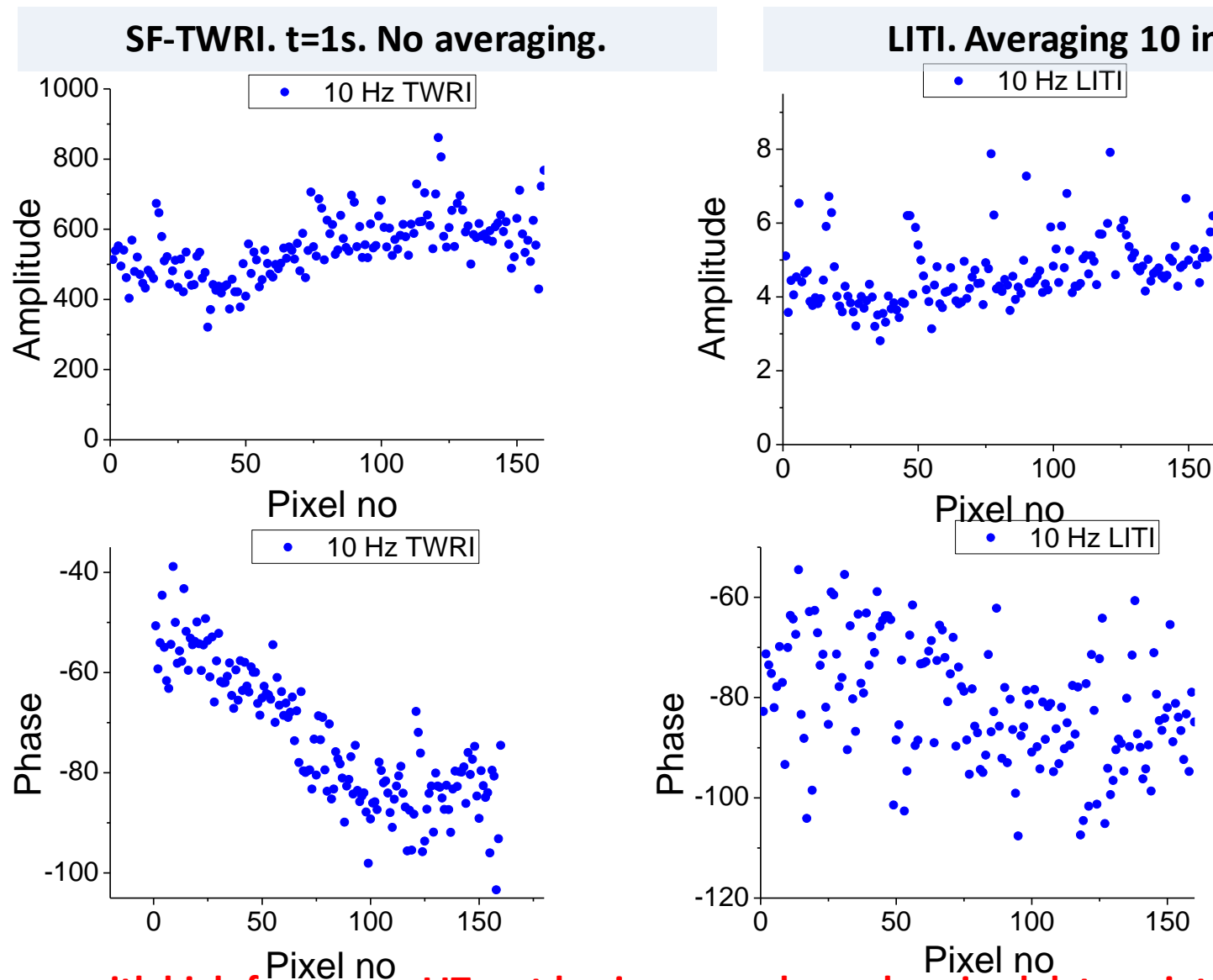
➤ Using the same frequency for the start and end of a TWRI sweep allows the calculation of the amplitude and phase at that frequency and the measurement of detailed pixel frequency dependencies by scanning over a wide range of frequencies at arbitrary intervals similar to photothermal radiometry, free from critical frequency exclusion, inter-frequency interval constraints, and upper limits imposed by sampling. **Signal processing is done through CC, not through the lock-in process.**

➤ **Critical parameters:** single-frequency chirp duration + (max) camera frame rate are operator controlled, *not controlled by frequency requirements.*

➤ **Result:** The SNR is higher for SF-TWR than for LIT and the SNR difference increases with increasing frequency.

➤ SF-TWR is advantageous for work requiring frequency scans (quantitative dynamic thermography)

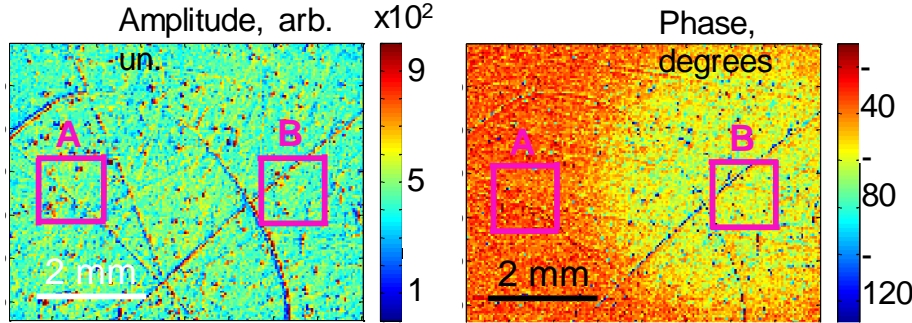
Comparison: LITI and SF-TWRI at 10 Hz for steel block with blind hole at 0.4 mm depth. Profiles of row 60.



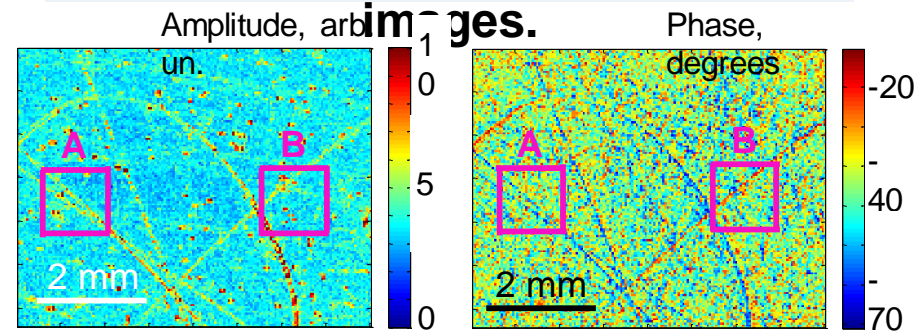
➤ Real issue with high frequency LIT: not having enough synchronized data points to process the lock-in method. This can be avoided with the chirp method at fixed frequencies.

Comparison: LITI and SF-TWRI at 16 Hz for steel block with blind hole at 0.4 mm depth. LITI undersampled by skipping 1 cycle.

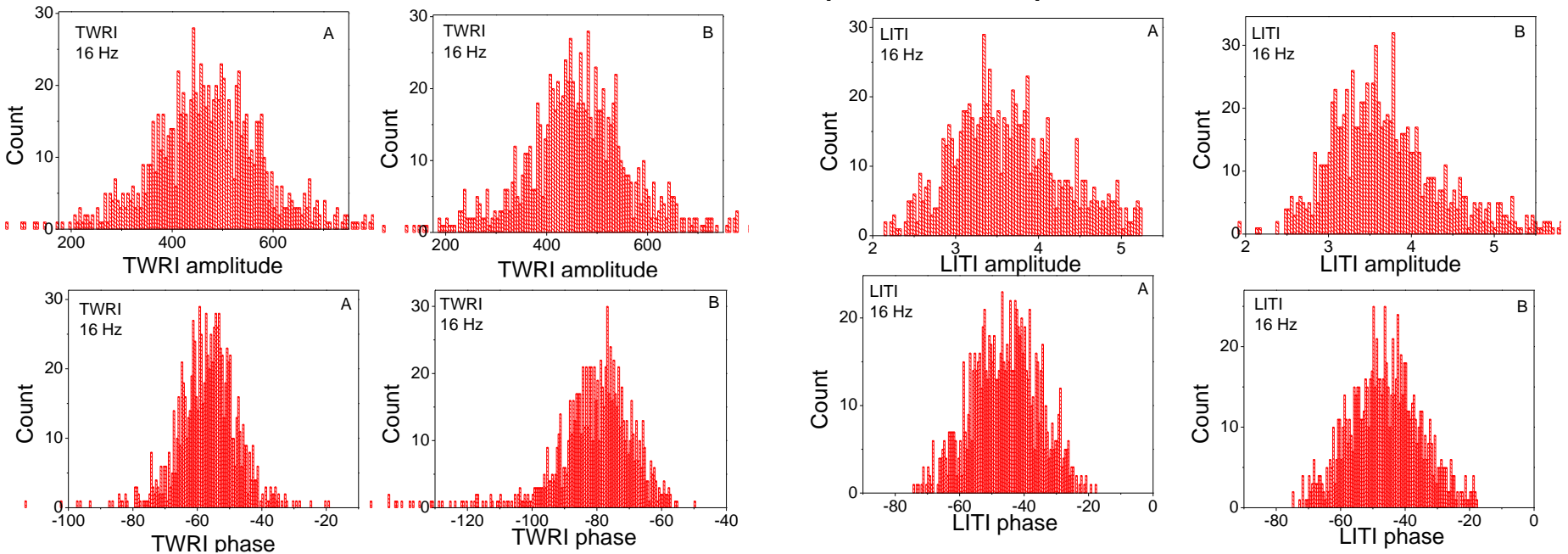
SF-TWRI. $t = 1$ s; 360 fr/s. $t = 1$ s.



LITI. 150 fr./s. Averaging 16

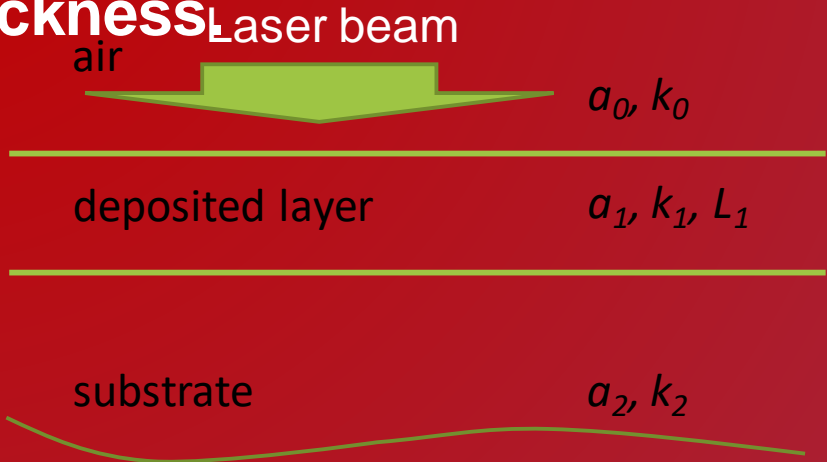


Statistical distributions of amplitude and phase for marked areas



- FWHM of amplitude and phase for SF-TWRI is less than for LITI.
- Depth resolution for TWRI is better than for LITI.

Quantitative SF-TWRI: Two - layer theoretical model with grouped parameters for quantitative estimation of layer thickness



Normalization by the semi-infinite substrate signal

$$\Delta T_1(0, f) = \frac{P_2(1 - \gamma_{01})}{P_1(1 - \gamma_{02})} \frac{(1 - \gamma_{21}e^{-2(i+1)\sqrt{\pi f}Q_1})}{(1 + \gamma_{21}e^{-2(i+1)\sqrt{\pi f}Q_1})}$$

Where

$$Q_m = \frac{L_m}{\sqrt{\alpha_m}}, \quad P_m = \frac{k_m}{\sqrt{\alpha_m}}, \quad \gamma_{mn} = \frac{b_{mn}-1}{b_{mn}+1},$$

$$b_{mn} = \frac{P_m}{P_n},$$

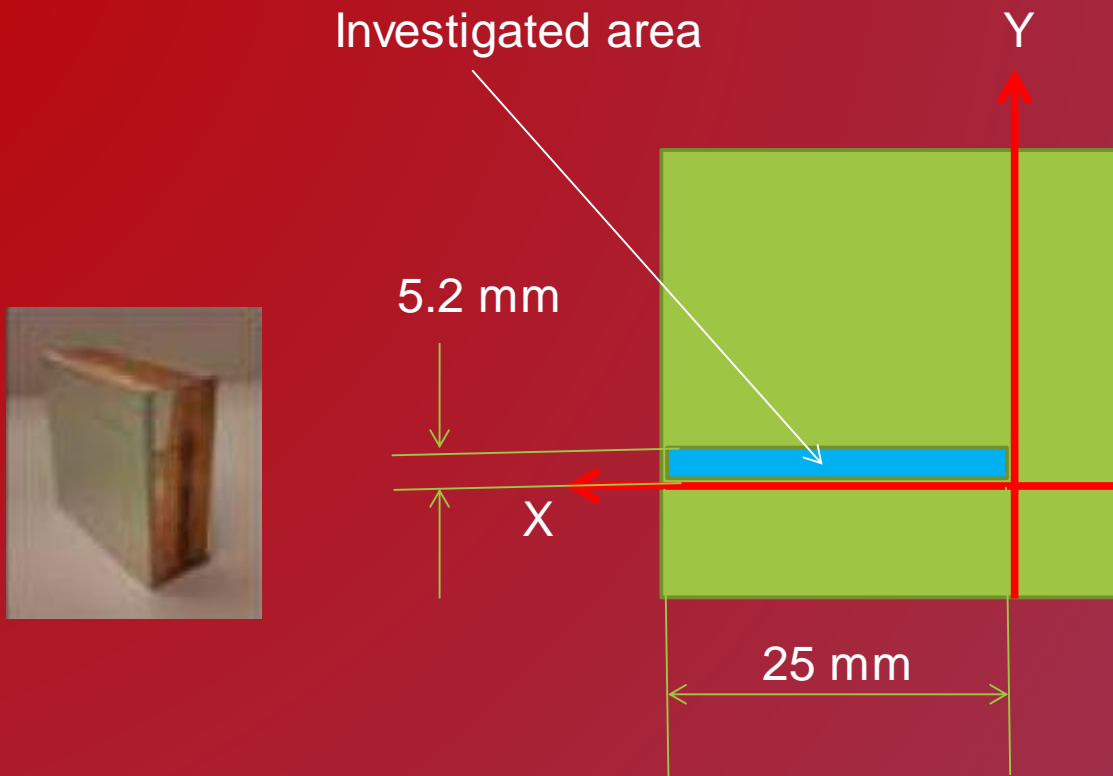
$$k_0 = 0.026 \text{ W m}^{-1}\text{k}^{-1}$$

$$\alpha_0 = 22.26 \cdot 10^{-6} \text{ m}^2/\text{s}$$

Parameters: Q_1, P_1, P_2

The Q parameter is the most sensitive parameter to layer thickness and is most reliably measured through frequency-response best-fitting.

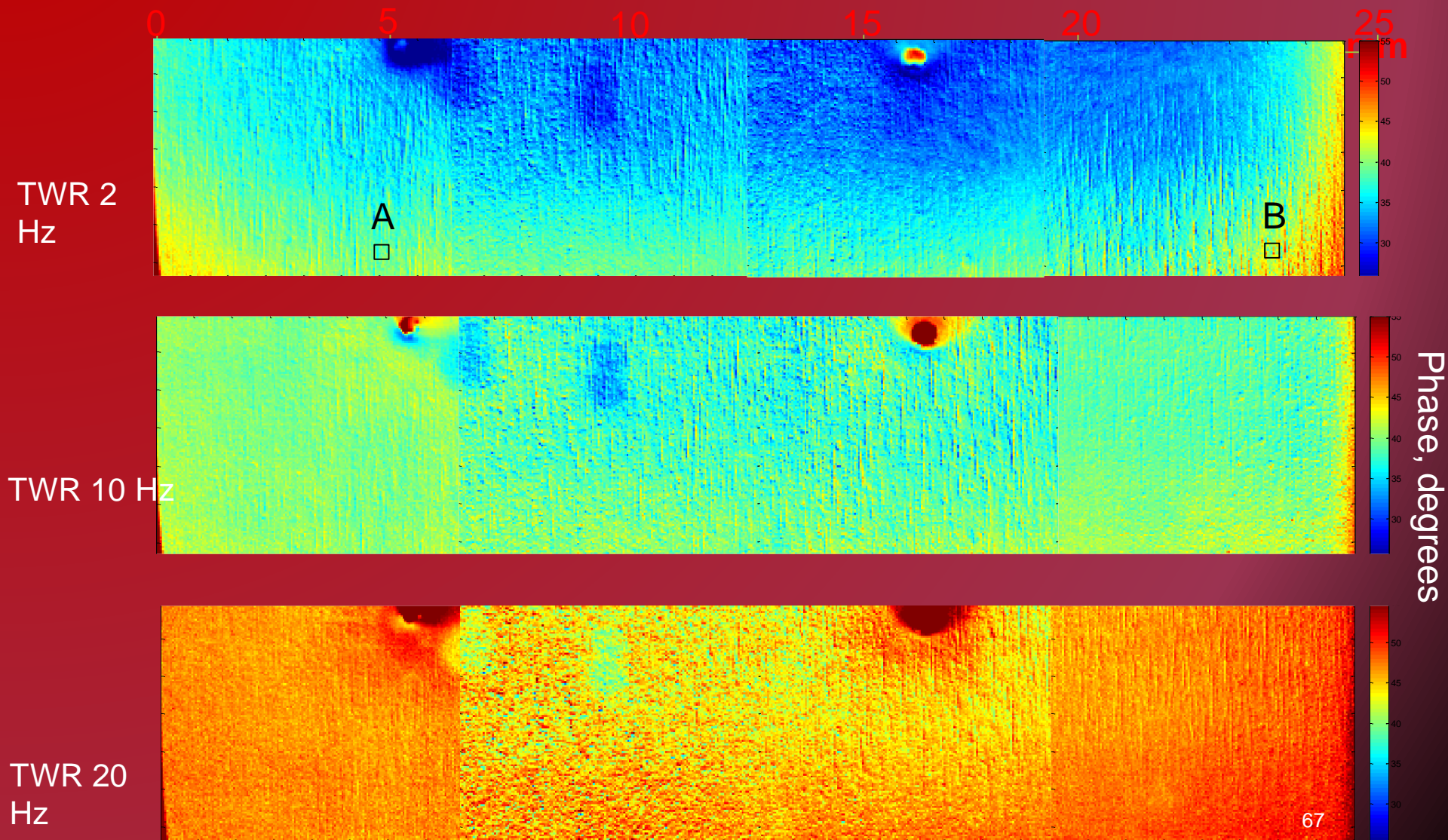
Sample for imaging of coating thickness (Al substrate)



~40 x 40 x 16 mm block

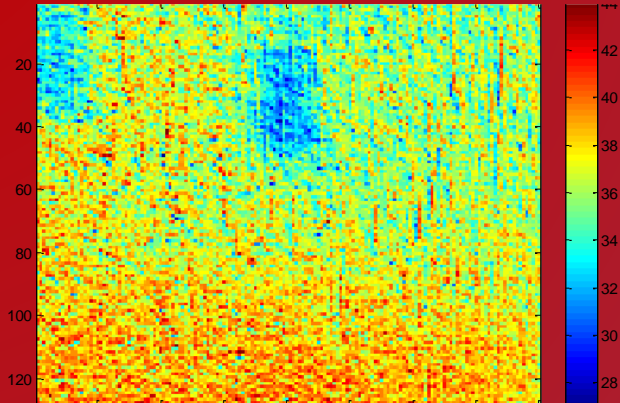
Al substrate, CoP nano-coating with nominal ~250 μm thickness

SF-TWR phase images of sample with deposited layer on the Al substrate.



Normalization procedure

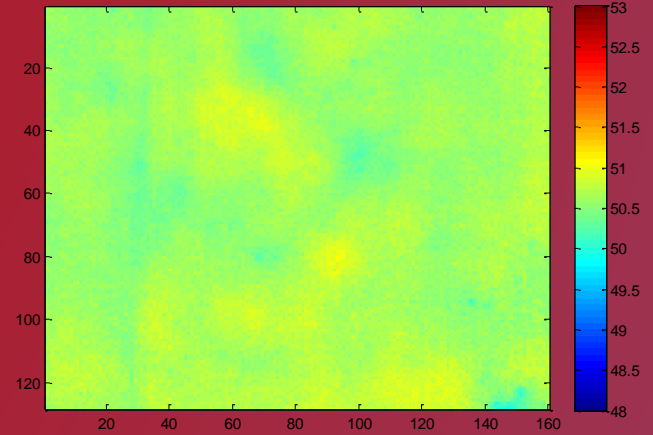
PHASE. 8HZ DEPOSITED LAYER
SAMPLE.



Normalization
to Zr sample

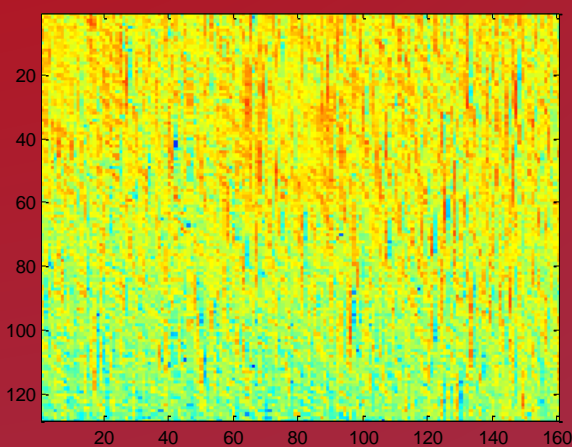


Phase. 8Hz. Zr



(phase of sample) – (phase of
Zr)

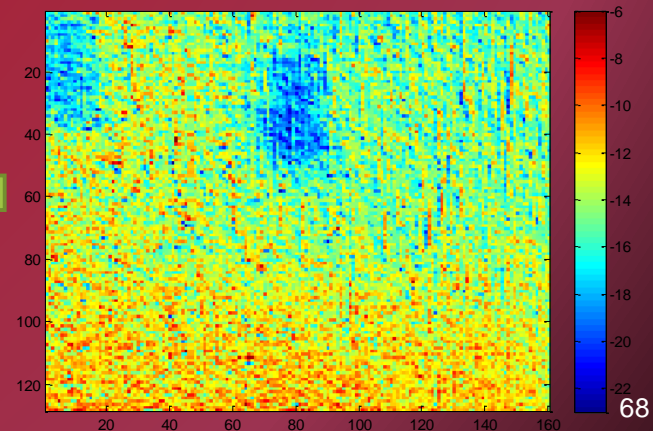
Fitted Q -
parameter

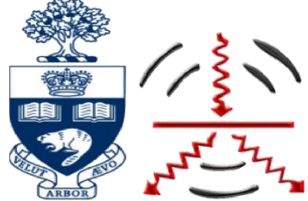


Fit to two-
layer model

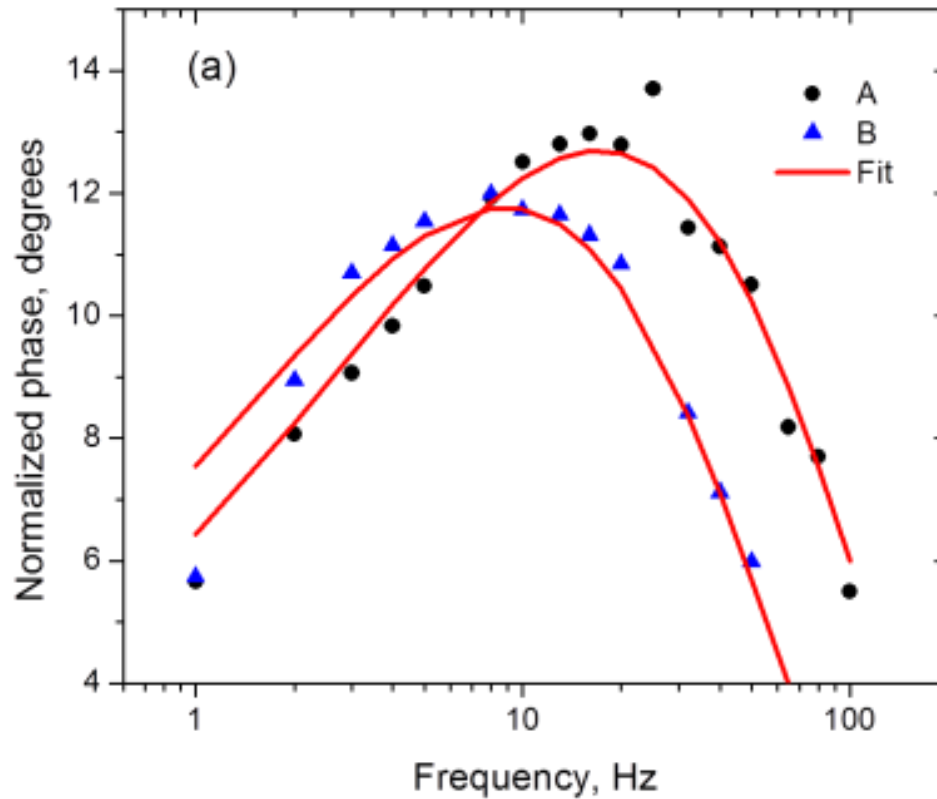


$$Q_1 = \frac{L_1}{\sqrt{\alpha_1}}$$



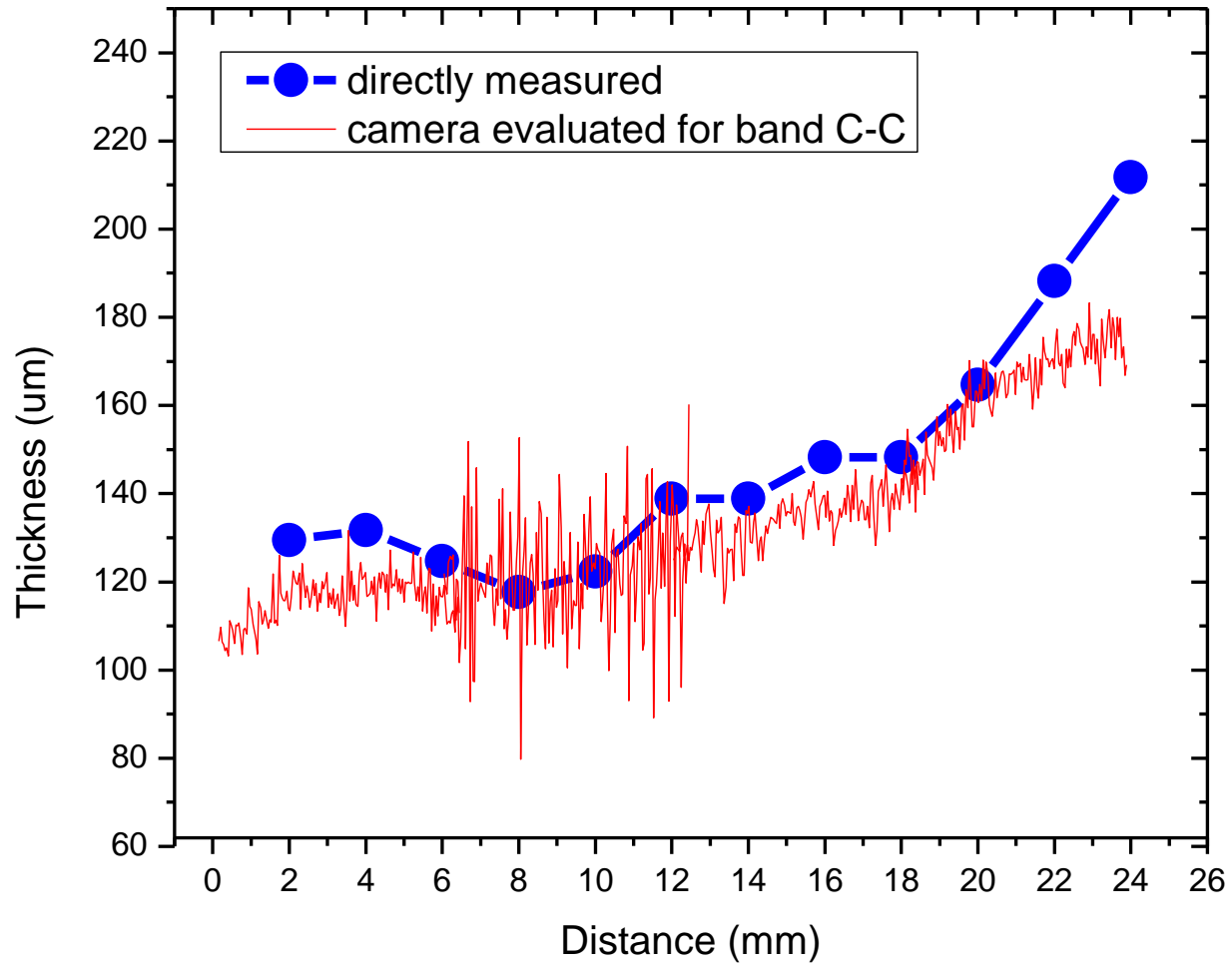


Normalized phase dependence on frequency for ROI A and B



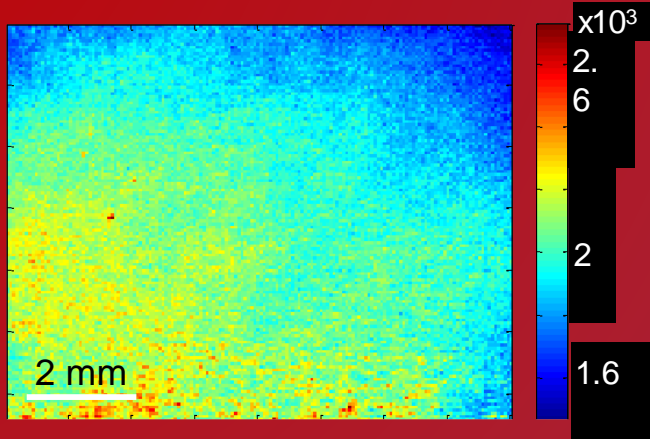
Phase was calculated as the mean value of a 6 x 6 pixel group in regions A and B. The frequency of phase maximum f_{max} is determined by parameter Q. Larger Q leads to f_{max} shift to lower frequency.

Directly measured and camera evaluated deposited layer thickness profiles

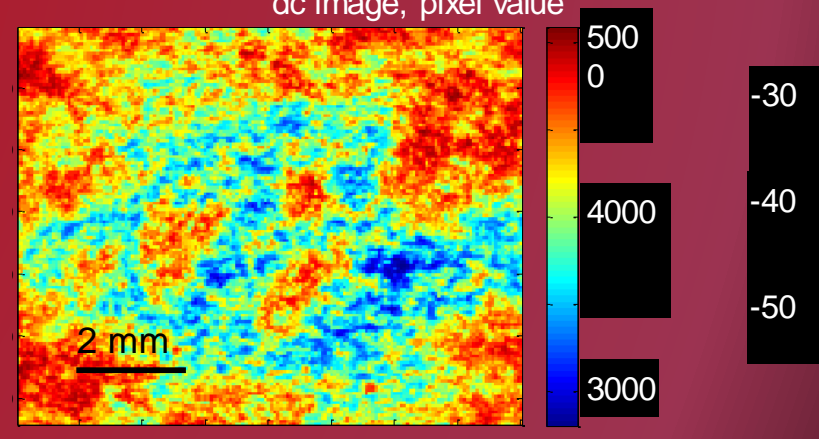


dc image and 20 Hz SF-TWR amplitude and phase images of sample with deposited layer on polymer (Polyetherketone, PEEK) substrate.

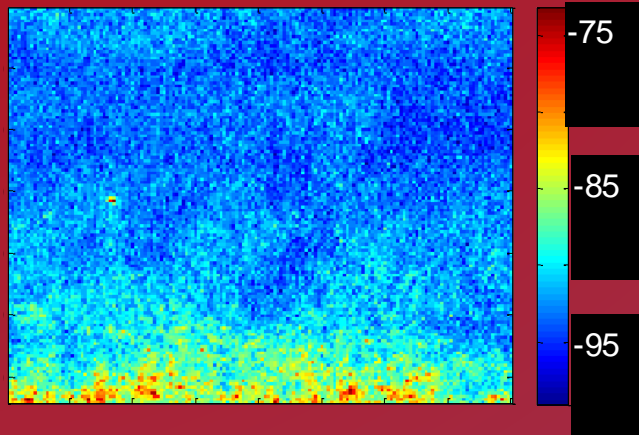
20 Hz amplitude, arb. un.



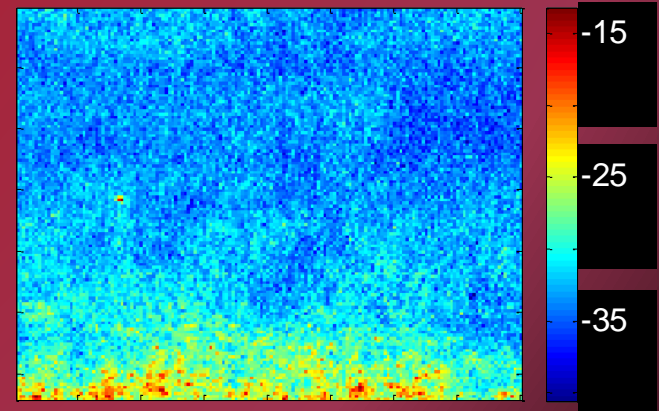
dc image, pixel value



20 Hz phase, degrees

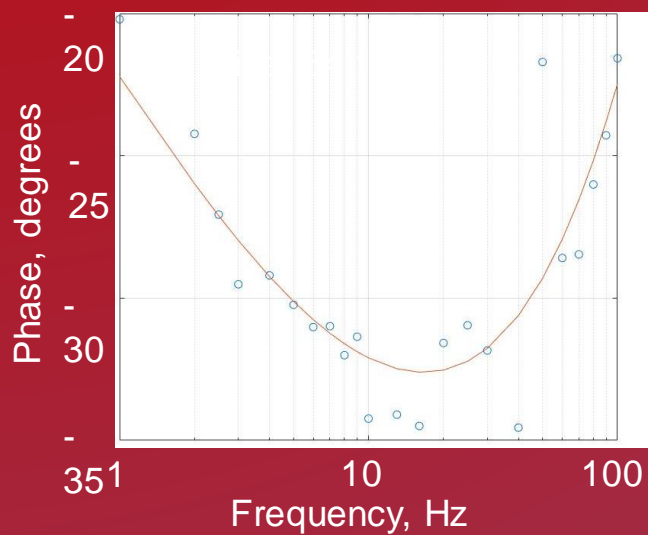
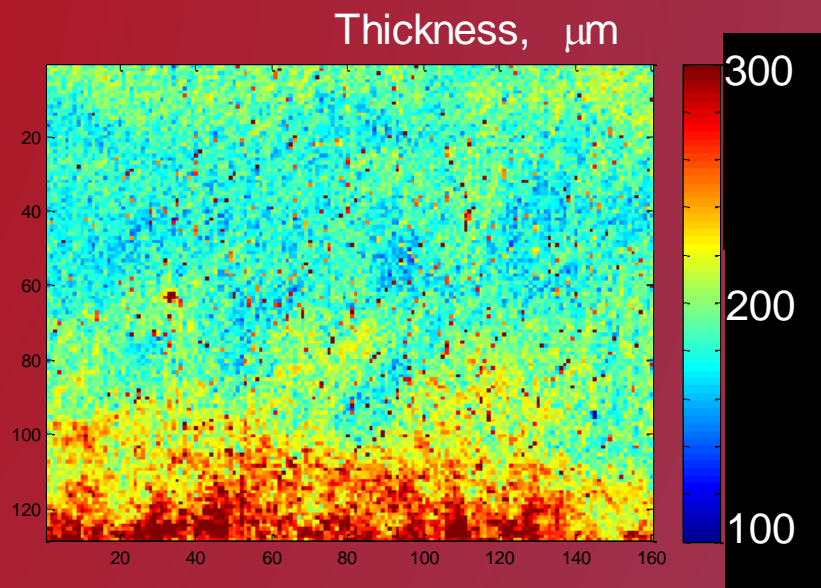
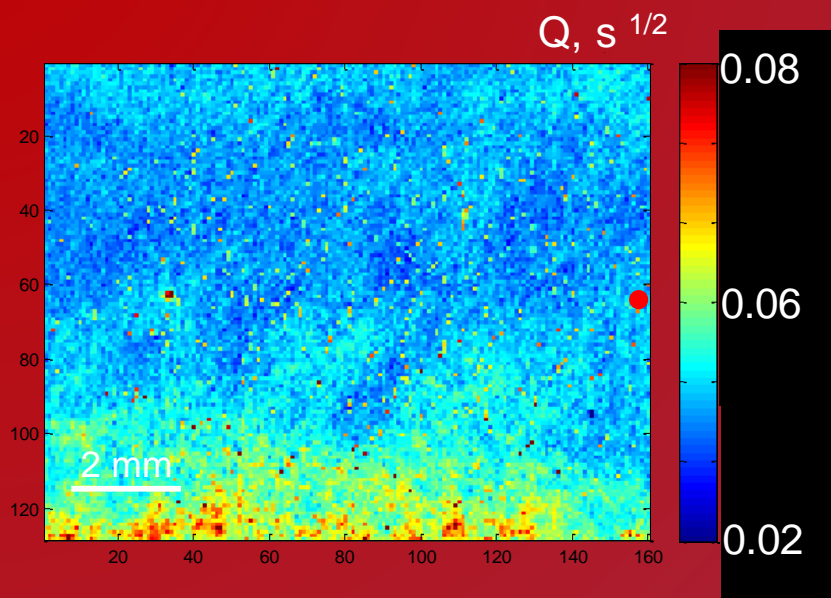


Phase, degrees



Normalization
with Zr sample

Images of Q-parameter and thickness of deposited layer on PEEK substrate.



Calculated α, m²/s	2.54E-05
Fitted Q, s^{1/2} (P64x160)	3.97E-02
Measured thickness (P64x160, μm)	200 μm

SUMMARY

- The temperature of an object can be determined based on the amount of infrared radiation it emits
- Thermal imaging cameras create a 2D image by detecting incoming radiation
- IR Cameras have a wide array of applications in the field of non-destructive testing and imaging
- **Passive Thermography** is established in building inspection, electrical and mechanical maintenance, optical gas imaging, Night Vision, Astronomy
- **Lock-in Thermography (LIT)** allows better contrast for inspection, is less sensitive to environmental conditions and has higher spatial resolution than passive thermography.
- Phase is less sensitive/insensitive to surface emissivity
- **Single-frequency (SF-) TWRI** is a next-generation dynamic quantitative thermography modality, an improvement over conventional LIT. It can be implemented at the same set-up as LIT with only software signal generation and processing change.
- The SNR is higher for SF-TWRI than for LIT and the SNR difference increases with increasing frequency.



Acknowledgments

- **Natural Sciences and Engineering Research Council of Canada (NSERC) - Discovery grant**
- **Canada Foundation for Innovation (CFI) - equipment grants**
- **Canada Research Chairs Program**



People. Discovery. Innovation.



Canada Research
Chairs

Chaires de recherche
du Canada